*Mathematical Biosciences and Engineering*

http://www.aimspress.com/journal/MBE

MBE, 18(1): 182–213.
DOI: 10.3934/mbe.2021010
Received: 31 August 2020
Accepted: 16 November 2020
Published: 26 November 2020

*Research article*

# A mathematical model for the impacts of face mask, hospitalization and quarantine on the dynamics of COVID-19 in India: deterministic vs. stochastic

**Akhil Kumar Srivastav[1], Pankaj Kumar Tiwari[2], Prashant K Srivastava[3], Mini Ghosh[1,*] and Yun Kang[4]**

[1] Division of Mathematics, School of Advanced Sciences, Vellore Institute of Technology, Chennai, India

[2] Department of Mathematics, University of Kalyani, Kalyani - 741235, India

[3] Department of Mathematics, Indian Institute of Technology Patna, Patna - 801103, India

[4] Science and Mathematics Faculty, Arizona State University Mesa, AZ 85212, USA

* **Correspondence:** Email: minighosh@vit.ac.in.

**Abstract:** In this paper, we propose a mathematical model to assess the impacts of using face masks, hospitalization of symptomatic individuals and quarantine of asymptomatic individuals in combating the COVID-19 pandemic in India. We calibrate the proposed model to fit the four data sets, viz. data for the states of Maharashtra, Delhi, Tamil Nadu and overall India, and estimate the rate of infection of susceptible with symptomatic population and recovery rate of quarantined individuals. We also estimate basic reproduction number to illustrate the epidemiological status of the regions under study. Our simulations infer that the infective population will be on increasing curve for Maharashtra and India, and settling for Tamil Nadu and Delhi. Sophisticated techniques of sensitivity analysis are employed to determine the impacts of model parameters on basic reproduction number and symptomatic infected individuals. Our results reveal that to curtail the disease burden in India, specific control strategies should be implemented effectively so that the basic reproduction number is decreased below unity. The three control strategies are shown to be important preventive measures to lower disease transmission rate. The model is further extended to its stochastic counterpart to encapsulate the variation or uncertainty observed in the disease transmissibility. We observe the variability in the infective population and found their distribution at certain fixed time, which shows that for small populations, the stochasticity will play an important role.

**Keywords:** COVID-19; deterministic and stochastic model; face mask; hospitalization; quarantine; parameter estimation; sensitivity analysis

## 1. Introduction

COVID-19 is wreaking havoc on the whole world at present, after its emergence in Wuhan in December 2019 and then global spread since February 2020. It has been categorized as pandemic by WHO. The disease, being caused by novel coronavirus (nCoV-SARS), is a new member of coronavirus family. Though researchers are actively involved in exploring the virus and its epidemiology, the knowledge about the disease is still very limited. This calls for scientific more studies to explore and understand the mechanism behind spread of virus and examine the impact of various pharmaceutical and non-pharmaceutical interventions. Mathematical modeling is one of the important tool for exploring the underlying dynamics of a disease spread and proposing control strategy when sufficient information about the disease is scarce. In an early study, Ferguson et al. [1] explored the impacts of two different non-pharmaceutical interventions, mitigation and suppression, and concluded that in case of mitigation, the implementation has to be for longer time period and also is less effective than suppression.

The spread of COVID-19 cases across 216 countries has brought the world under serious threat [2]. As people patiently wait through the lockdowns imposed across different countries for the development of an effective treatment strategy and the invention of a vaccine, it becomes imperative to forecast the COVID-19 cases for designing effective strategies and policy to fight the pandemic, and heal the scars that it is leaving behind on lives of the people as well as on the global economy [3].

SARS-CoV-2 is similar to the other respiratory pathogens in which airborne transmission occurs by inhaling droplets loaded with SARS-CoV-2 particles that are emitted from infectious people when speaking, coughing or sneezing [4, 5]. This is most likely to occur in poorly ventilated areas where droplets or mist particles can accumulate and be inhaled [6–8]. Infection can also occur through the mucous membranes of the head (eyes, nose and mouth), when SARS-CoV-2 particles are picked up on the hands and then transferred to the head by face-touching behaviours. Strict adherence to physical distancing, good hand hygiene, and trace and track have been weaponized to decrease the cumulative number of registered COVID-19 cases. Such control measures can make significant delay to attain the epidemic peak.

Medical or surgical face masks are associated with a higher degree of protection by blocking the spread of respiratory droplets. This simple and inexpensive practice may significantly reduce the global economic recession in this pandemic crisis. It is also possible that this low-level technology could reduce the severe global economic impact of COVID-19 [9]. Stutt et al. [10] showed that use of face masks in public could serve as a control measure to prevent inter-human transmission. The findings of Chu et al. [11] suggested that optimum use of face masks, N95 or similar respirators, and eye protection in public and health-care settings could confer additional benefit to decrease viral exposure.

The study of Ngonghala et al. [12] showed that the use of surgical face masks with efficacy more than 70% in public could lead to the elimination of the pandemic if at least 70% of the residents of New York state consistently use such masks in public. Eikenberry et al. [13] showed that broad adoption of even relatively ineffective face masks may reduce community transmission of COVID-19 and decrease peak hospitalizations and deaths. Moreover, mask use decreases the effective transmission rate in nearly linear proportion to the product of mask effectiveness and coverage rate, while the impact on epidemiologic outcomes is highly nonlinear, indicating masks could synergize with other non-pharmaceutical measures. Iboi et al. [14] showed that COVID-19 can be efficiently

controlled using social-distancing measures provided its effectiveness level is at least moderate; the use of face masks in the public can significantly reduce COVID-19 in Nigeria, its use as a sole intervention strategy may fail to lead to the realistic elimination of the disease. The eradication of disease requires unrealistic high compliance in face mask usage in the public, in the range of 80% to 95%. However, the findings of Okuonghae and Omame [15] showed that if at least 55% of the population comply with the social distancing regulation and effectively making use of face masks while in public, the disease will eventually die out. In addition, stepping up the case detection rate for symptomatic individuals lead to a great decrease in the prevalence of COVID-19. Hand hygiene and facemasks seemed to prevent household transmission of influenza virus when implemented within 36 hours of index patient symptom onset [16]. Public-health efforts to reduce transmission are expected to have a substantial impact on reducing the size of COVID-19 pandemic [17]. Through an imitating social learning process, individual-level behavioral change on taking infection prevention actions have the potentials to significantly reduce the COVID-19 outbreak in terms of size and timing at city-level [18]. Timely and substantially resources and supports for improving the willingness-to-act and conducts of self-administered infection prevention actions can reduce the risks associated with COVID-19.

Mathematical models have been proposed to explore the efficiency of hospital isolation of the confirmed infected person, quarantine of people contacting them, and home containment of all population to restrict mobility, lockdowns on the dynamics of COVID-19. The assumption is that all infected individuals are isolated after the incubation period. Findings of Khoshnaw et al. [19] suggested that healthcare programs should pay more attention to intervention strategies, and people need to self-quarantine and that can effectively reduce the disease. Serhani and Labbardi [20] have shown that home containment, if strictly followed, plays a crucial role in controlling the spread of COVID-19.

In this paper, we propose a mathematical model for the dynamics of COVID-19 in India. In the model, we also account for the natural birth and deaths in the population. We classify the infective population into two subcategories − symptomatic and asymptomatic. We assume that as soon as symptoms appear, an asymptomatic individual joins the class of symptomatic populations. Further, we consider that the asymptomatic individuals will be home quarantined, an important consideration in the modeling of COVID-19. Our model focuses on the impacts of face mask, hospitalization of symptomatic individuals and quarantine of asymptomatic individuals on the transmission dynamics of COVID-19 pandemic in India. We study the effectiveness of these three control measures on flattening the disease progress curve. Our aim is to investigate whether these three control strategies can eliminate the burden of COVID-19 in India? These epidemiological questions will be answered by model analysis and simulation results. The basic difference between our model and existing models is that we provide a comprehensive and robust study of impact of above mentioned interventions on the spread of COVID-19 in India. Our study provides a mathematical model and its analysis, estimation of parameters with help of data and then sustainable sensitivity of parameters via stochastic extension of the model.

Remainder of the paper is organized in the following way: section 2 contains model formulation and underlying assumptions. In the following section, we obtain disease-free and endemic equilibria of the system. Analytical expression for the basic reproduction number is obtained using the next generation matrix method. Further, sufficient conditions are derived for the global stability of the

endemic equilibrium. We simulate our model in Section 4. The model is calibrated using daily COVID-19 cases of three states of India, namely Maharshtra, Delhi and Tamil Nadu, and the whole country. Sensitivity analysis is performed to identify parameters having crucial roles in disease control. In Section 5, we extend our deterministic model to a corresponding stochastic model. The stochastic system is analyzed and simulated, and the obtained results are compared with the corresponding deterministic system. Finally, the results are compiled and discussed in closing section, conclusion.

## 2. The mathematical model

Here, we formulate a compartmental model for dynamics of COVID-19 in India by considering human-to-human transmission of the disease [21]. We divide the total human population $N$, into seven compartments: susceptible individuals $S$, exposed individuals $E$, symptomatic individuals $I_s$, asymptomatic individuals $I_a$, hospitalized individuals $H$, home quarantined asymptomatic individuals $Q_h$ and recovered individuals $R$. Thus, we have $N = S + E + I_s + I_a + H + Q_h + R$. It should be emphasized that the compartment $I_a$ also contains individuals who may show mild symptoms of the disease but are not recognized as COVID-19 infected individuals. Furthermore, the compartment $H$ for hospitalization also includes those with clinical symptoms of COVID-19 who are self-isolating at home. Descriptions of all the dynamical variables of the considered model are given in Table 1.

**Table 1.** Descriptions of variables used in the model system (2.1).

| Variables | Descriptions |
|---|---|
| $S$ | Number of susceptible human population |
| $E$ | Number of exposed human population |
| $I_s$ | Number of symptomatic human population |
| $I_a$ | Number of asymptomatic human population |
| $H$ | Number of hospitalized and/or notified human population |
| $Q_h$ | Number of quarantined human population |
| $R$ | Number of recovered human population |

For developing the mathematical model, we make the following assumptions.

1. The individuals are recruited in the region at a constant rate $\Lambda$ and join the susceptible class.
2. The susceptible individuals become exposed to the infection and join the exposed class on effective contacts with symptomatic and asymptomatic infectious human population at the rates $\beta_1$ and $\beta_2$, respectively.
3. A proportion $c_m$ of population wear face masks correctly and consistently in public places. Let $\epsilon_m$ be the efficacy of the face masks. The proper use of face masks reduces disease transmission effectively [14]. So, the above effective disease transmission rates $\beta_1$ and $\beta_2$ modify to $\beta_1(1-\epsilon_m c_m)$ and $\beta_2(1-\epsilon_m c_m)$, respectively.
4. A fraction of exposed individuals show clinical symptoms and join the symptomatic class while the remaining move to the asymptomatic class. Some of the asymptomatic individuals show clinical symptoms with passage of time and join the symptomatic class at the rate $\alpha_a$.

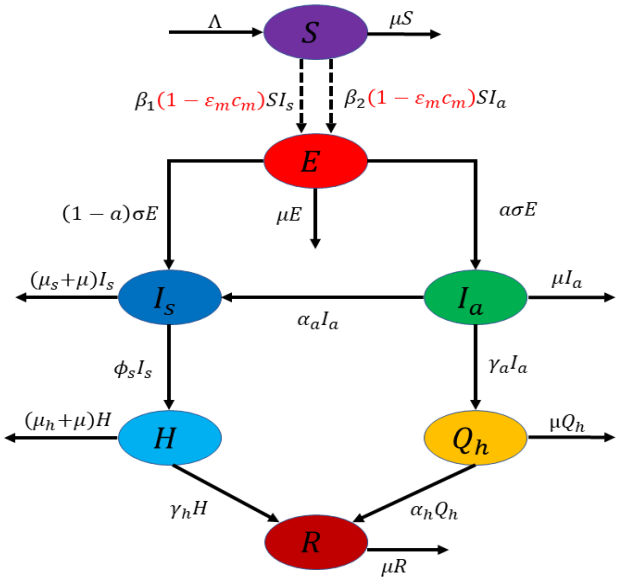


**Figure 1.** Schematic diagram of the model (2.1). Here, black dashed arrow represents new infection term, one sided arrow indicates progression to other compartments, and red color stands for the impacts of face masks in reducing transmission rates from symptomatic and asymptomatic humans to susceptible individuals.

5. The symptomatic individuals are hospitalized at the rate $\phi_s$ while the individuals in asymptomatic class move to the quarantined compartment at the rate $\gamma_a$.
6. The hospitalized and quarantined individuals recover from COVID-19 at the rates $\gamma_h$ and $\alpha_h$, respectively.
7. The symptomatic and hospitalized individuals can proceed to severe complications of COVID-19 and experience COVID-19-induced mortality at the rates $\mu_s$ and $\mu_h$, respectively. Humans in each class have natural mortality.
8. The recovered individuals do not acquire the infection again and are not going to infect others.

In view of these assumptions, a schematic diagram is given in Figure 1, and the corresponding model equations are as follows:

$$\begin{aligned}
\frac{dS}{dt} &= \Lambda - \beta_1(1-\epsilon_m c_m)S\,I_s - \beta_2(1-\epsilon_m c_m)S\,I_a - \mu S,\\
\frac{dE}{dt} &= \beta_1(1-\epsilon_m c_m)S\,I_s + \beta_2(1-\epsilon_m c_m)S\,I_a - \sigma E - \mu E,\\
\frac{dI_s}{dt} &= (1-a)\sigma E + \alpha_a I_a - (\mu_s+\mu)I_s - \phi_s I_s,\\
\frac{dI_a}{dt} &= a\sigma E - \gamma_a I_a - \alpha_a I_a - \mu I_a,\\
\frac{dH}{dt} &= \phi_s I_s - (\gamma_h + \mu_h + \mu)H,\\
\frac{dQ_h}{dt} &= \gamma_a I_a - \alpha_h Q_h - \mu Q_h,
\end{aligned} \tag{2.1}$$

$$\frac{dR}{dt} = \alpha_h Q_h + \gamma_h H - \mu R.$$

System (2.1) is analyzed with positive initial conditions. Here, $0 \leq a, \epsilon_m, c_m \leq 1$. The effects of wearing face masks in public can be measured by the overall reduction in the baseline values of the community contact rate parameters $\beta_1$ and $\beta_2$. Note that $\beta_1 \neq \beta_2$ represents the possible heterogeneity in the contact rates of infectious with or without clinical symptoms of COVID-19. Also, we assume that $\beta_1 \geq \beta_2$. All the parameters involved in system (2.1) are assumed to be constants and have non-negative real values. The descriptions of model's parameters are given in Table 2.

**Table 2.** Descriptions of parameters involved in the system (2.1).

| Parameters | Descriptions | Units |
|---|---|---|
| $\Lambda$ | Recruitment rate in the susceptible class | persons day$^{-1}$ |
| $\beta_1$ | Rate of infection of susceptible with symptomatic human | person$^{-1}$day$^{-1}$ |
| $\beta_2$ | Rate of infection of susceptible with asymptomatic human | person$^{-1}$day$^{-1}$ |
| $\epsilon_m$ | Efficacy of face masks | — |
| $c_m$ | Masks compliance | — |
| $\sigma$ | Rate of incubation | day$^{-1}$ |
| $a$ | Fraction of exposed individuals not showing clinical symptoms | — |
| $\alpha_a$ | Rate of progression from asymptomatic to symptomatic class | day$^{-1}$ |
| $\phi_s$ | Rate of hospitalization of symptomatic individuals | day$^{-1}$ |
| $\gamma_a$ | Quarantine rate of asymptomatic individuals | day$^{-1}$ |
| $\gamma_h$ | Recovery rate of hospitalized individuals | day$^{-1}$ |
| $\alpha_h$ | Recovery rate of quarantined individuals | day$^{-1}$ |
| $\mu$ | Natural death rate of humans | day$^{-1}$ |
| $\mu_s$ | Disease induced mortality rate for symptomatic individuals | day$^{-1}$ |
| $\mu_h$ | Disease induced mortality rate for hospitalized individuals | day$^{-1}$ |

## 3. Mathematical analysis of the system (2.1)

### *3.1. Positivity and boundedness of the solutions*

From the model system (2.1), we have

$$\left.\frac{dS}{dt}\right|_{S=0} = \Lambda > 0, \ \left.\frac{dE}{dt}\right|_{E=0} = \beta_1(1-\epsilon_m c_m)S I_s + \beta_2(1-\epsilon_m c_m)S I_a > 0,$$
$$\left.\frac{dI_s}{dt}\right|_{I_s=0} = (1-a)\sigma E + \alpha_a I_a \geq 0, \ \left.\frac{dI_a}{dt}\right|_{I_a=0} = a\sigma E \geq 0, \ \left.\frac{dH}{dt}\right|_{H=0} = \phi_s I_s \geq 0,$$
$$\left.\frac{dQ_h}{dt}\right|_{Q_h=0} = \gamma_a I_a \geq 0, \ \left.\frac{dR}{dt}\right|_{R=0} = \alpha_h Q_h + \gamma_h H \geq 0.$$

Here, all the rates are non-negative on the bounding planes. So, if we start in the interior of the 7-dimensional closed hyperoctant $\mathbb{R}^7_+$, we will always remain there, in view of the fact that the direction of the vector field is inward on all the bounding planes. Thus, non-negativity of all the solutions of the model system (2.1) is guaranteed.

Further, from the model system (2.1), we note that the total human population $N$ satisfies,

$$\frac{dN}{dt} = \Lambda - \mu N - \mu_s I_s - \mu_h H.$$

This gives,

$$\limsup_{t\to\infty} N \leq \frac{\Lambda}{\mu}.$$

Therefore, all the solutions $S(t)$, $E(t)$, $I_s(t)$, $I_a(t)$, $H(t)$, $Q_h(t)$ and $R(t)$ are bounded by $\Lambda/\mu$. Hence, the biologically feasible region for the system (2.1) is given by the following positively invariant set:

$$\Omega_1 = \{(S, E, I_s, I_a, H, Q_h, R) \in \mathbb{R}^7_+ : 0 \leq S, E, I_s, I_a, H, Q_h, R \leq \Lambda/\mu\}.$$

3.1.1. Disease-free equilibrium and its stability

The model system (2.1) has the disease-free equilibrium $E_0 = (\Lambda/\mu, 0, 0, 0, 0, 0, 0)$, which is always feasible.

Using next-generation matrix method [22], we determine the expression for basic reproduction number ($\mathcal{R}_0$), an index worldwide commonly used by public health organizations as a key estimator of the severity of a given epidemic. The new infection terms and transition terms of the system (2.1) are respectively given by

$$\mathcal{F} = \begin{pmatrix} \beta_1(1-\epsilon_m c_m)S I_s + \beta_2(1-\epsilon_m c_m)S I_a \\ 0 \\ 0 \end{pmatrix},$$

$$\mathcal{V} = \begin{pmatrix} (\sigma+\mu)E \\ -(1-a)\sigma E - \alpha_a I_a + (\phi_s + \mu_s + \mu)I_s \\ -a\sigma E + (\gamma_a + \alpha_a + \mu)I_a \end{pmatrix}.$$

Now, we find the matrices $F$ (of new infection terms) and $V$ (of the transition terms) as

$$F = \begin{pmatrix} 0 & \beta_2(1-\epsilon_m c_m)\frac{\Lambda}{\mu} & \beta_1(1-\epsilon_m c_m)\frac{\Lambda}{\mu} \\ 0 & 0 & 0 \\ 0 & 0 & 0 \end{pmatrix},$$

$$V = \begin{pmatrix} \sigma+\mu & 0 & 0 \\ -(1-a)\sigma & -\alpha_a & \phi_s + \mu_s + \mu \\ -a\sigma & \gamma_a + \alpha_a + \mu & 0 \end{pmatrix}.$$

It follows that

$$FV^{-1} = \begin{pmatrix} \widehat{a}_{11} & \widehat{a}_{12} & \widehat{a}_{13} \\ 0 & 0 & 0 \\ 0 & 0 & 0 \end{pmatrix},$$

where

$$\widehat{a}_{11} = \frac{\beta_1\Lambda(1-\epsilon_m c_m)\{\alpha_a\sigma + \sigma(1-a)(\gamma_a+\mu)\}}{\mu(\mu+\sigma)(\alpha_a+\gamma_a+\mu)(\mu+\mu_s+\phi_s)} + \frac{\beta_2 a\sigma\Lambda(1-\epsilon_m c_m)}{\mu(\mu+\sigma)(\alpha_a+\gamma_a+\mu)},$$

$$\widehat{a}_{12} = \frac{\beta_1\Lambda(1-\epsilon_m c_m)}{\mu(\mu+\mu_s+\phi_s)},\ \widehat{a}_{13} = \frac{\beta_2\Lambda(1-\epsilon_m c_m)}{\mu(\gamma_a+\alpha_a+\mu)} + \frac{\beta_1\alpha_a\Lambda(1-\epsilon_m c_m)}{\mu(\gamma_a+\alpha_a+\mu)(\mu+\mu_s+\phi_s)}.$$

The basic reproduction number is same as the spectral radius of the next-generation matrix $FV^{-1}$. Thus, from above, we obtain the expression for $\mathcal{R}_0$ as

$$\mathcal{R}_0 = \frac{\Lambda\sigma(1-\epsilon_m c_m)}{\mu(\mu+\sigma)(\alpha_a+\gamma_a+\mu)}\left[\frac{\beta_1\{\alpha_a+(1-a)(\gamma_a+\mu)\}}{\mu+\mu_s+\phi_s}+\beta_2 a\right].$$

The quantity $\mathcal{R}_0$ is known as basic reproduction number, the expected number of secondary cases produced in completely susceptible population, by a typical infective individual for the system (2.1). From the expression of basic reproduction number, it is apparent that the value of $\mathcal{R}_0$ decreases with increase in the efficacy and compliance of face masks. Instead, the immigration of people and transmission rates of COVID-19 from symptomatic/asymptomatic individuals to susceptible individuals boost up the value of $\mathcal{R}_0$. Moreover, if the face masks are 100% efficient to control disease transmission and are supplied in sufficiently large quantity, i.e., $\epsilon_m = c_m = 1$, the value of $\mathcal{R}_0$ becomes zero and in that case the disease will not be transmitted from one person to another person.

The following local stability result of the disease-free equilibrium $E_0$ follows from [22].

**Theorem 3.1.** *For model system (2.1), the disease-free equilibrium $E_0$ is locally asymptotically stable if $\mathcal{R}_0 < 1$ and unstable if $\mathcal{R}_0 > 1$.*

### *3.2. Endemic equilibrium and its stability*

**Theorem 3.2.** *The model system (2.1) has a unique endemic equilibrium $E_1 = (S^*, E^*, I_s^*, I_a^*, H^*, Q_h^*, R^*)$ which exists only if $\mathcal{R}_0 > 1$. The components of $E_1$ are:*

$$\begin{aligned}
&S^* = \frac{\Lambda}{\beta_1(1-\epsilon_m c_m)I_s^* + \beta_2(1-\epsilon_m c_m)I_a^* + \mu},\ I_a^* = \frac{a\sigma E^*}{\gamma_a+\alpha_a+\mu},\ I_s^* = \frac{(1-a)\sigma E^* + \alpha_a * I_a^*}{\phi_s+\mu_s+\mu},\\
&H^* = \frac{\phi_s I_s^*}{\gamma_h+\mu_h+\mu},\ Q_h^* = \frac{\gamma_a I_a^*}{\alpha_h+\mu},\ R^* = \frac{\alpha_h Q_h^* + \gamma_h H^*}{\mu},\\
&E^* = \left[\frac{(\phi_s+\mu_s+\mu)(\gamma_a+\alpha_a+\mu)}{\sigma(\sigma+\mu)(1-\epsilon_m c_m)[\beta_1\{(1-a)(\gamma_a+\mu)+\alpha_a\}+\beta_2 a(\phi_s+\mu_s+\mu)]}\right]\\
&\quad\times\left[\frac{\Lambda\sigma(1-\epsilon_m c_m)[\beta_1\{(1-a)(\gamma_a+\mu)+\alpha_a\}+\beta_2 a(\phi_s+\mu_s+\mu)]}{(\phi_s+\mu_s+\mu)(\gamma_a+\alpha_a+\mu)} - (\sigma+\mu)\mu\right]\\
&\quad= \frac{(\mathcal{R}_0-1)(\gamma_a+\alpha_a+\mu)(\phi_s+\mu_s+\mu)}{\sigma(\sigma+\mu)(1-\epsilon_m c_m)[\beta_1\{(1-a)(\gamma_a+\mu)+\alpha_a\}+\beta_2 a(\phi_s+\mu_s+\mu)]}.
\end{aligned}$$

*Proof.* The proof follows by equating the right hand side of differential equations in system (2.1) to zero and solving these algebraic equations. □

In the following, we establish global stability of the unique endemic equilibrium $E_1$.

**Theorem 3.3.** *The endemic equilibrium $E_1$ exists if $\mathcal{R}_0 > 1$, and is globally asymptotically stable inside the region of attraction $\Omega_1$ if the following conditions are satisfied:*

$$\frac{\beta_1 S^*}{\mu_s+\mu+\phi_s} < \frac{\epsilon_m c_m(\sigma+\mu)}{3\sigma(1-a)}, \tag{3.1}$$

$$\frac{\beta_2 S^*}{\gamma_a+\alpha_a+\mu} < \frac{\epsilon_m c_m(\sigma+\mu)}{3\sigma a}, \tag{3.2}$$

$$\frac{\beta_1\alpha_a^2}{1-a} < \frac{\beta_2(\gamma_a+\alpha_a+\mu)(\mu_s+\mu+\phi_s)}{a}, \tag{3.3}$$

$$\frac{\sigma(1-\epsilon_m c_m)^2 S^*}{\epsilon_m c_m \mu}\max\left\{\frac{1-a}{\mu_s+\mu+\phi_s}, \frac{a}{\gamma_a+\alpha_a+\mu}\right\} < \frac{4\mu(\sigma+\mu)}{27}\left[\frac{\mu}{\Lambda(\beta_1+\beta_2)(1-\epsilon_m c_m)}\right]^2. \tag{3.4}$$

*Proof.* To establish the global stability of endemic equilibrium $E_1$, we consider the following positive definite function

$$\begin{aligned} U &= \frac{1}{2}(S-S^*)^2+\frac{1}{2}m_1(E-E^*)^2+\frac{1}{2}m_2(I_s-I_s^*)^2+\frac{1}{2}m_3(I_a-I_a^*)^2+\frac{1}{2}m_4(H-H^*)^2 \\ &\quad +\frac{1}{2}m_5(Q_h-Q_h^*)^2+\frac{1}{2}m_6(R-R^*)^2, \end{aligned} \tag{3.5}$$

where $m_i$'s ($i = 1-6$) are positive constants to be chosen appropriately.

Differentiating Eq (3.5) with respect to time along the solutions of system (2.1), and choosing $m_2 = m_1\dfrac{\beta_1\epsilon_m c_m S^*}{\sigma(1-a)}$ and $m_3 = m_1\dfrac{\beta_2\epsilon_m c_m S^*}{\sigma a}$, we have

$$\begin{aligned} \frac{dU}{dt} &= -[\beta_1(1-\epsilon_m c_m)I_s+\beta_2(1-\epsilon_m c_m)I_a+\mu](S-S^*)^2-m_1(\sigma+\mu)(E-E^*)^2 \\ &\quad -m_1\frac{\beta_1\epsilon_m c_m S^*}{(1-a)\sigma}(\mu_s+\mu+\phi_s)(I_s-I_s^*)^2-m_1\frac{\beta_2\epsilon_m c_m S^*}{a\sigma}(\gamma_a+\mu+\alpha_a)(I_a-I_a^*)^2 \\ &\quad -m_4(\gamma_h+\mu_h+\mu)(H-H^*)^2-m_5(\alpha_h+\mu)(Q_h-Q_h^*)^2-m_6\mu(R-R^*)^2 \\ &\quad +m_1\beta_1 S^*(I_s-I_s^*)(E-E^*)+m_1\beta_2 S^*(I_a-I_a^*)(E-E^*)-\beta_1(1-\epsilon_m c_m)S^*(I_s-I_s^*)(S-S^*) \\ &\quad -\beta_2(1-\epsilon_m c_m)S^*(I_a-I_a^*)(S-S^*)+m_1[\beta_1(1-\epsilon_m c_m)I_s+\beta_2(1-\epsilon_m c_m)I_a](S-S^*)(E-E^*) \\ &\quad +m_1\frac{\beta_1\epsilon_m c_m S^*\alpha_a}{(1-a)\sigma}(I_a-I_a^*)(I_s-I_s^*)+m_4\phi_s(I_s-I_s^*)(H-H^*)+m_5\gamma_a(I_a-I_a^*)(Q_h-Q_h^*) \\ &\quad +m_6\alpha_h(R-R^*)(Q_h-Q_h^*)+m_6\gamma_h(R-R^*)(H-H^*). \end{aligned}$$

Thus, $\dfrac{dU}{dt}$ will be negative definite inside the region of attraction $\Omega_1$, if the following inequalities hold:

$$\frac{\beta_1 S^*}{\mu_s+\mu+\phi_s} < \frac{1}{3}\frac{\epsilon_m c_m(\sigma+\mu)}{(1-a)\sigma}, \tag{3.6}$$

$$\frac{\beta_2 S^*}{\gamma_a+\alpha_a+\mu} < \frac{1}{3}\frac{\epsilon_m c_m(\sigma+\mu)}{a\sigma}, \tag{3.7}$$

$$\frac{\beta_1\alpha_a^2}{1-a} < \frac{\beta_2}{a}(\gamma_a+\alpha_a+\mu)(\mu_s+\mu+\phi_s), \tag{3.8}$$

$$\beta_1(1-\epsilon_m c_m)^2 S^* < \frac{m_1}{3}\frac{\epsilon_m c_m\mu}{(1-a)\sigma}(\mu_s+\mu+\phi_s), \tag{3.9}$$

$$\beta_2(1-\epsilon_m c_m)^2 S^* < \frac{m_1}{3}\frac{\epsilon_m c_m\mu}{a\sigma}(\gamma_a+\alpha_a+\mu), \tag{3.10}$$

$$m_1\left[\frac{(\beta_1+\beta_2)(1-\epsilon_m c_m)\Lambda}{\mu}\right]^2 < \frac{4}{9}(\sigma+\mu)\mu, \tag{3.11}$$

$$m_4\phi_s^2 < \frac{m_1}{2}\frac{\beta_1\epsilon_m c_m S^*}{(1-a)\sigma}(\gamma_h+\mu_h+\mu), \tag{3.12}$$

$$m_5\gamma_a^2 < \frac{m_1}{2}\frac{\beta_2\epsilon_m c_m S^*}{a\sigma}(\gamma_a+\alpha_a+\mu)(\alpha_h+\mu), \tag{3.13}$$

$$m_6\alpha_h^2 < \frac{2m_5}{3}\mu(\alpha_h+\mu), \tag{3.14}$$

$$m_6\gamma_h^2 < \mu m_4(\gamma_h+\mu_h+\mu). \tag{3.15}$$

From inequalities (3.9)–(3.11), we have

$$\frac{3\sigma(1-\epsilon_m c_m)^2 S^*}{\epsilon_m c_m \mu}\max\left\{\frac{1-a}{\mu_s+\mu+\phi_s}, \frac{a}{\gamma_a+\alpha_a+\mu}\right\} < \frac{4\mu(\sigma+\mu)}{9}\left[\frac{\mu}{(\beta_1+\beta_2)(1-\epsilon_m c_m)\Lambda}\right]^2.$$

From inequality (3.12), we obtain

$$0 < m_4 < \frac{m_1}{2\phi_s^2}\frac{\beta_1\epsilon_m c_m S^*}{(1-a)\sigma}(\gamma_h+\mu_h+\mu).$$

From inequality (3.13), we obtain

$$0 < m_5 < \frac{m_1}{2\gamma_a^2}\frac{\beta_2\epsilon_m c_m S^*}{a\sigma}(\gamma_a+\alpha_a+\mu)(\alpha_h+\mu).$$

From inequalities (3.14) and (3.15), we have

$$0 < m_6 < \min\left\{\frac{2m_5\mu(\alpha_h+\mu)}{3\alpha_h^2}, \frac{\mu m_4(\gamma_h+\mu_h+\mu)}{\gamma_h^2}\right\}.$$

We note that $\frac{dU}{dt}$ is negative definite inside the region of attraction $\Omega_1$ if the inequalities (3.1)–(3.4) hold.

□

## 4. Numerical simulation

### *4.1. Data and model calibration*

For the purpose of parameter estimation, we have used data of COVID-19 active cases from India and its three states, Maharashtra, Delhi and Tamil Nadu for the time period March to June, 2020. The choice of these three states is motivated by the fact that these are among the most affected regions in India. The different time stamp data are used. For example, we used 10th March 2020 to 25th June 2020 for Maharashtra, 5th March 2020 to 25th June 2020 for Delhi, 17th March 2020 to 25th June 2020 for Tamil Nadu, and 1st March 2020 to 25th June 2020 for India for our study. These COVID-19 active cases data was collected from [23]. The daily data pattern of total active cases for Maharastra, Delhi, Tamil Nadu and India during the study period are provided in Figure 2. Here, it should be noted that day one in each plot match with first date of the data. For example, day one for Maharashtra is 10th March while for Delhi it is 5th March.

We now estimate the infection rate of COVID-19 of susceptible with symptomatic population ($\beta_1$) and the recovery rate of self-quarantined humans ($\alpha_h$) for these three states and the whole country. In addition, we also estimate the basic reproduction number for these four data sets. For the purpose of parameter estimation, we use the values of rest of parameters either from available sources or they are suitably assumed. The values of these parameters are provided in Table 3.

**Table 3.** Values of parameters in model system (2.1).

| Parameters | Values | References |
|---|---|---|
| $\Lambda$ | Varies | |
| $\beta_2$ | 0.000513 | Assumed |
| $\epsilon_m$ | 0.5 | [25] |
| $c_m$ | 0.1 | [26] |
| $\sigma$ | [0.071,0.33] | [27,28] |
| $a$ | [0.15,0.7] | [1,28] |
| $\gamma_a$ | 0.2 | [12] |
| $\gamma_h$ | 1/14 | [29,30] |
| $\mu$ | 0.000425 | Demographic |
| $\mu_h$ | 0.0042 | Assumed |
| $\alpha_a$ | [0.01,0.08] | [31] |
| $\phi_s$ | [0.02,0.1] | [1,28] |
| $\mu_s$ | 0.0052 | Assumed |

The R−software is used to fit the simulated and observed COVID-19 active cases for all these four data sets during the mentioned time period using maximum likelihood method. A detailed discussion on this model fitting technique is provided in [24]. The estimated values of parameters and the basic reproduction number for all these four data sets are given in Table 4. From the table, we note that the estimated value of the transmission of disease between symptomatic and susceptible individuals ($\beta_1$) is highest in Maharashtra along with the largest value of the basic reproduction number ($\mathcal{R}_0$). The reason behind this could be high population density, improper lock-down, lack of social distancing and inefficient use of preventive measures in the state. On the other hand, $\beta_1$ is low for overall population of India. We also observe that the basic reproduction number is least for Tamil Nadu. This will lead to relatively slow progression of the disease. The table also shows that Delhi has relatively highest recovery rate for quarantine population. The estimated values of $\mathcal{R}_0$ for France, UK, Singapore, Germany, Spain and Japan were found to be 3.5, 2.9, 1.7, 3.5, 3.5 and 1.7, respectively during the initial phase of disease transmission [32]. Note that the estimated value of $\mathcal{R}_0$ for India is greater than Singapore and Japan, but lower than those of France, UK, Germany and Spain. The model fitting is provided in Figure 3 with real COVID-19 data for all four data sets. In the figure, red dots represent the observed active COVID-19 case data and solid curve stands for the corresponding fitted curve from the proposed model system; the shaded regions indicate 95% confidence intervals.

Further, we are interested to know how the disease will progress as time passes, i.e., we are interested in short term prediction. For this purpose, we use the estimated parameters for respective data sets, keeping other parameters at the same values as in Table 3, and simulated our model for 160 days. The observed active COVID-19 case data for all four data sets is plotted with red dots and

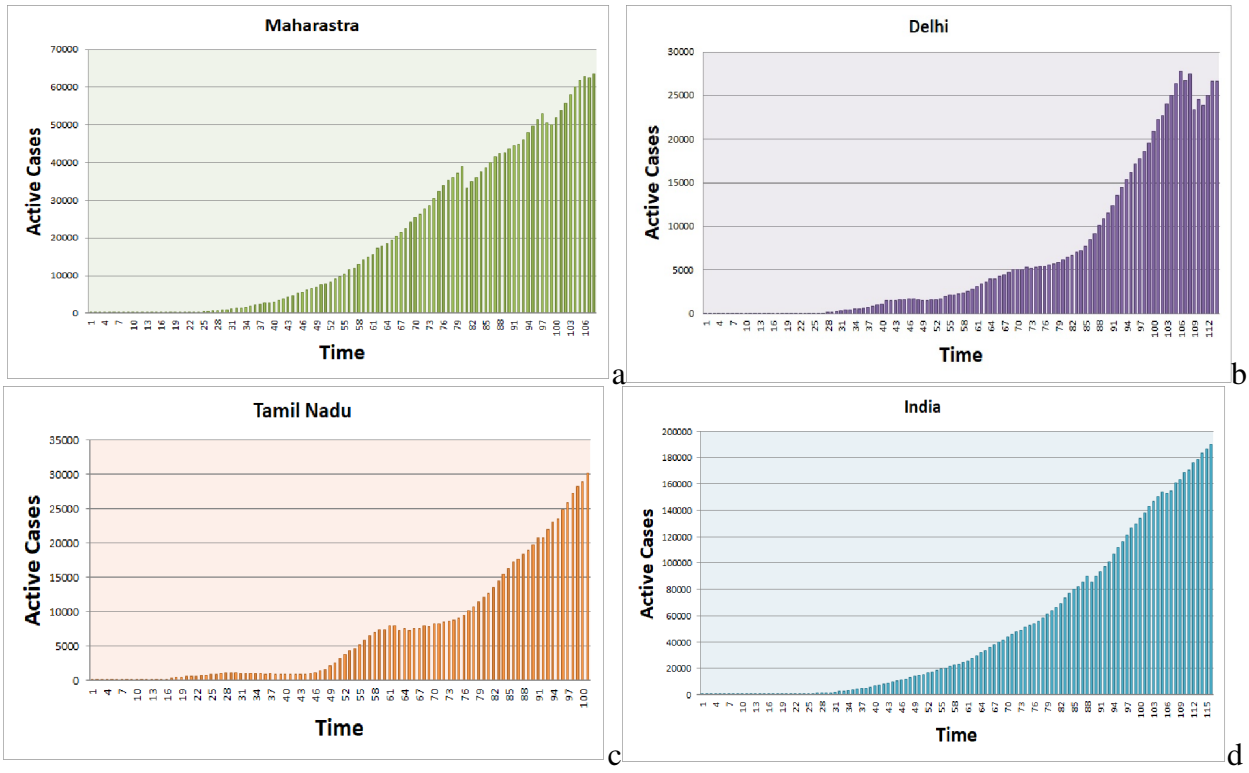


**Figure 2.** Active COVID-19 cases for (a) Maharastra, (b) Delhi, (c) Tamil Nadu and (d) India during study period.

**Table 4.** Mean values of estimated parameters $\beta_1$ and $\alpha_h$, and the basic reproduction number ($\mathcal{R}_0$) in 95% confidence interval.

| States | Estimated values of parameters | Estimated values of $\mathcal{R}_0$ |
|---|---|---|
| Maharastra | $\beta_1 = 0.065$ | 2.568 |
| | $\alpha_h = 0.0019$ | |
| Delhi | $\beta_1 = 0.054$ | 2.315 |
| | $\alpha_h = 0.0025$ | |
| Tamil Nadu | $\beta_1 = 0.049$ | 1.892 |
| | $\alpha_h = 0.00022$ | |
| India | $\beta_1 = 0.037$ | 2.183 |
| | $\alpha_h = 0.00145$ | |

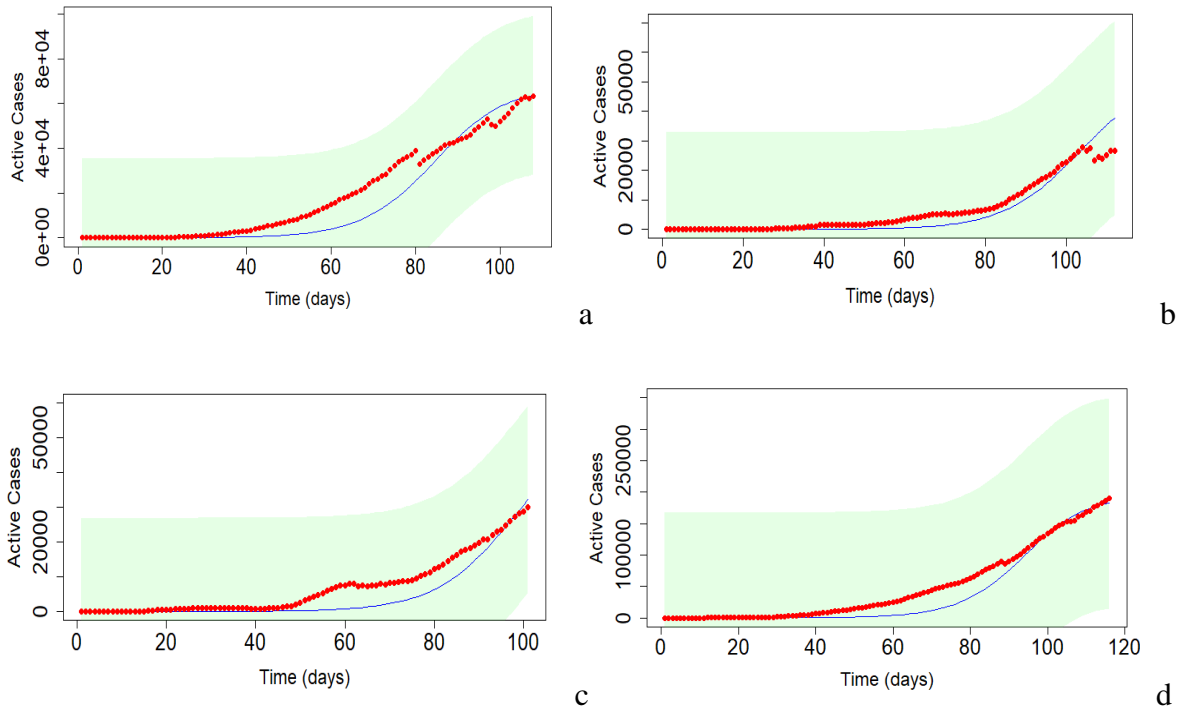


**Figure 3.** Plots of the output of the fitted model (2.1) and the observed active COVID-19 cases for (a) Maharastra, (b) Delhi, (c) Tamil Nadu and (d) India. Red dotted line shows real data points and the blue line stands for model solution. Shaded regions indicate 95% confidence interval.

the solid curve shows the model prediction, Figure 4. It can be noted from Figures 4(a) & 4(d), that our model predicts increase in number of active COVID-19 positive cases for the state of Maharashtra and overall India. However, from Figures 4(b) & 4(c), we can note that the predicted curve is bending, which means that the active cases will start to saturate and may further reduce after the last date of data for these data sets. We must underline that these predictions solely depend on current practices and will be valid provided there is no sudden control measure adopted by the respective state governments or central government. The prediction for long term is neither feasible nor appropriate given the dynamic and ever evolving nature of disease and interventions.

### *4.2. Impacts of parameters on basic reproduction number*

We establish the normalized forward sensitivity indices of the basic reproduction number with respect to model parameters [33]. The normalized forward sensitivity index of a variable to a parameter describes the ratio of the relative change in the variable to the relative change in the parameter. In Figure 5, we plot the sensitivity indices of $\mathcal{R}_0$ with respect to the parameters of interest. Evidently, Figure 5 suggests that the magnitude of $\mathcal{R}_0$ increases with increase in the values of parameters $\Lambda$, $\beta_1$, $\beta_2$ and $\sigma$ as these parameters possess positive indices with $\mathcal{R}_0$. Similarly, the parameters having negative indices with $\mathcal{R}_0$ are $\epsilon_m$, $c_m$, $\alpha_a$, $\gamma_a$, $\mu$, $\mu_s$, $a$ and $\phi_s$. Hence, increments in these parameters cause decline in the value of $\mathcal{R}_0$. We find that for the parameter $\Lambda$, the sensitivity

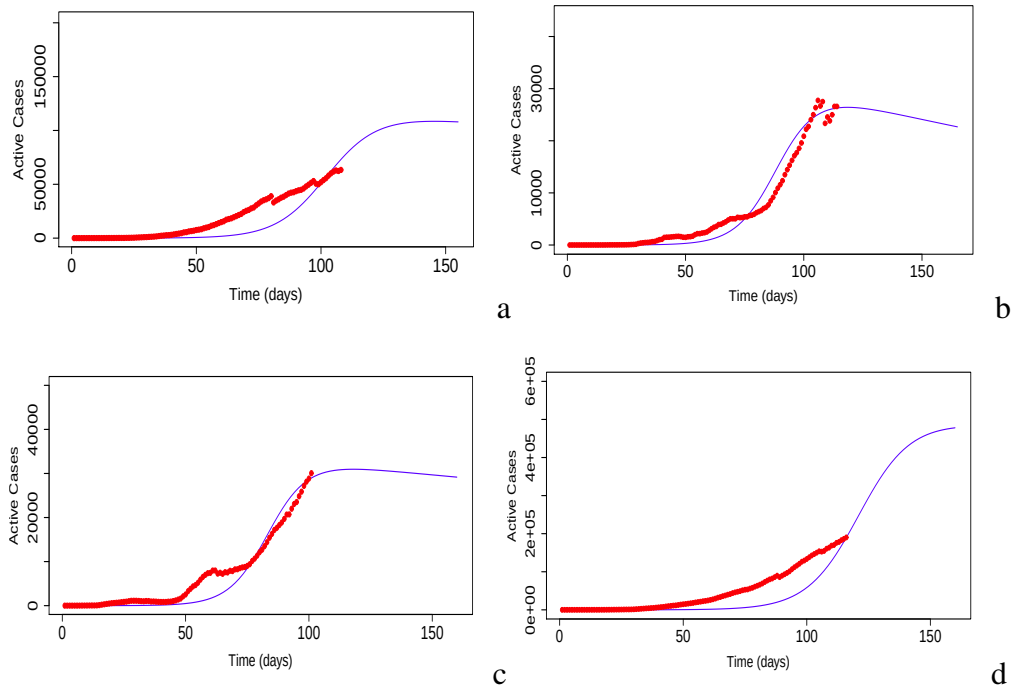


**Figure 4.** Plots of the output of the fitted model (2.1) and the observed active COVID-19 cases with prediction for (a) Maharastra, (b) Delhi, (c) Tamil Nadu and (d) India. Red dotted line shows data points and blue line shows model solution.

index of $\mathcal{R}_0$ is 1. It means that 1% increase in the value of $\Lambda$ will result in 1% increase in the value of $\mathcal{R}_0$. It is clear that occurrence of a lower value of $\mathcal{R}_0$ helps to prevent the disease prevalence. Thus, to wipe out the disease from the system, we must control the increase of the parameters having positive indices with basic reproduction number whereas parameters which have negative indices should be sustained. Therefore, any prevention measure which can reduce the disease burden must be seriously considered by the health-care officials to control the subsequent outbreaks. We find that the control parameters such as use of protective masks, quarantine and hospitalization efficacy etc., which are negatively correlated with $\mathcal{R}_0$ should be implemented by means of proper hygiene and efficient health-care services.

As pointed out in the introduction, now, we are interested to see the impacts of masks compliance and efficacy of face masks ($c_m$ and $\epsilon_m$) on the basic reproduction number ($\mathcal{R}_0$) for India and its three most affected states: Maharastra, Delhi and Tamil Nadu. For this, we plot the values of $\mathcal{R}_0$ with respect to $\epsilon_m$ and $c_m$ (see Figure 6). The contour plots show that the epidemic potential can be drawn below unity for higher efficacy and compliance of face masks. For lower transmission rates of COVID-19 infection of susceptible with symptomatic population, the values of $\mathcal{R}_0$ remain below unity and rise in rate of hospitalization of symptomatic individuals lead to further reductions in the values of $\mathcal{R}_0$, Figure 7. The quarantine of asymptomatic individuals also significantly reduces the epidemic potential $\mathcal{R}_0$, Figure 8. The public health implications of these are that, COVID-19 can be controlled effectively and will be eventually die out from the Indian states by compulsory face masks wearing in public, hospitalization of symptomatic individuals and quarantine of asymptomatic individuals.

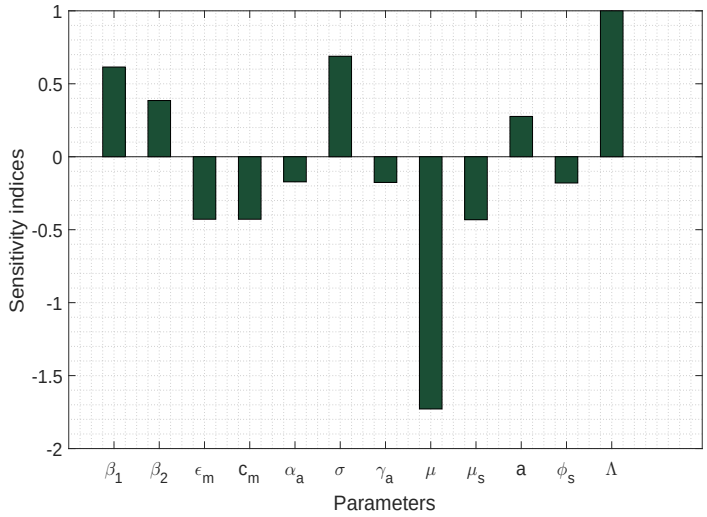


**Figure 5.** Normalized forward sensitivity indices of $\mathcal{R}_0$ with respect to model parameters. Parameter values: $\beta_1 = 0.03$, $\beta_2 = 0.003$, $\Lambda = 50000$, $\epsilon_m = 0.5$, $c_m = 0.6$, $\mu = 0.00042$, $\sigma = 0.00019$, $\mu_s = 0.06$, $\alpha_a = 0.004$, $\alpha_h = 0.0002$, $\gamma_a = 0.002$, $\phi_s = 0.025$, $\gamma_h = 0.071$, $\mu_h = 0.05$, $a = 0.4$.

### *4.3. Impacts of parameters on disease prevalence*

By using the method of [34, 35], we perform global sensitivity analysis of system (2.1). We pick some epidemiologically important controllable parameters: $\Lambda, \beta_1, \beta_2, \epsilon_m, c_m, \gamma_a, \alpha_h, \gamma_h$ and $\phi_s$ as input parameters and symptomatic infective population, $I_s$, as response function. Two statistical techniques are applied in the process: Latin Hypercube Sampling (LHS) and Partial Rank Correlation Coefficients (PRCCs). The former supports to vary several parameters together in a systematic way while the latter interlink the input parameters and response function allocating values between $-1$ and 1. Notably, the sign of PRCC describes the type of correlations between input parameters and the response function whereas its values mean strength. Nonlinear and monotone relationships were recognized between symptomatic infective population and the input parameters, which is an essential condition for computing PRCCs. We consider an uniform distribution for each input parameter and run 200 simulations per LHS. The parameters are supposed to deviate ±25% from their nominal values. The PRCC values are plotted in Figure 9, which depicts that the parameters $\Lambda, \beta_1$ and $\beta_2$ have positive correlations with symptomatic infective population whereas the parameters having negative impacts on symptomatic infective population are $\epsilon_m, c_m, \gamma_a, \alpha_h, \gamma_h$ and $\phi_s$. Out of these parameters, only $\Lambda$, $\gamma_a$ and $\phi_s$ show significant correlations with the symptomatic infective population characterized by having $p-$value less than 0.05. Determination of the correlation between input parameters and the response function helps to develop effective control strategies to declutter the COVID-19 burden. The sensitivity results suggest that the prevention measures of COVID-19 should be: prompted hospitalization of symptomatic individuals and proper quarantine of asymptomatic individuals to reduce the spread of COVID-19. Also, making the habit of using face mask sincerely, can minimize the risk of disease transmission. Growing density of the recovery class is also important for excising the disease from the environment.

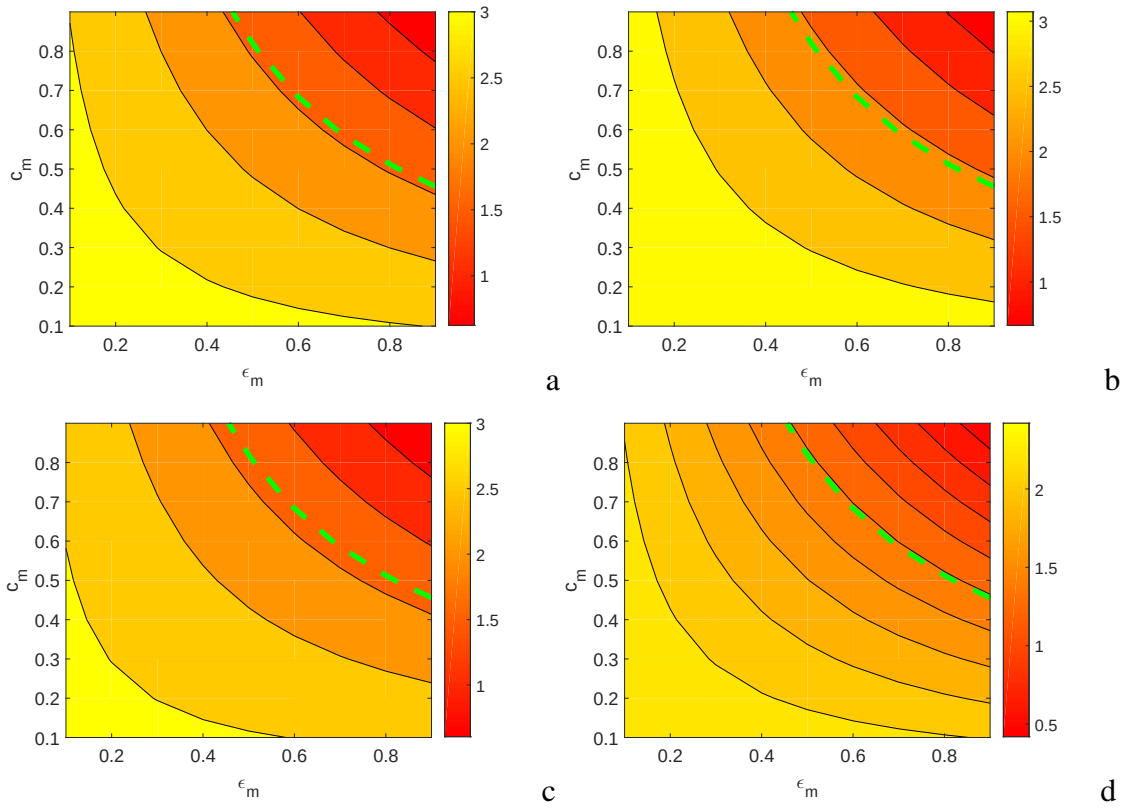


**Figure 6.** Contour plots of the basic reproduction number ($\mathcal{R}_0$) with respect $\epsilon_m$ and $c_m$ for (a) Maharashtra, (b) Delhi, (c) Tamil Nadu and (d) India. The dashed green line represents $\mathcal{R}_0 = 1$. Parameter values: $\beta_2 = 0.00003$, $\mu = 0.0042$, $\sigma = 0.000019$, $\mu_s = 0.06$, $\alpha_a = 0.0004$, $\gamma_a = 0.2$, $\phi_s = 0.025$, $\gamma_h = 0.071$, $\mu_h = 0.05$, $a = 0.4$; in (a) $\beta_1 = 0.065$, $\Lambda = 7$, $\alpha_h = 0.0019$, (b) $\beta_1 = 0.054$, $\Lambda = 9$, $\alpha_h = 0.0025$, (c) $\beta_1 = 0.049$, $\Lambda = 9$, $\alpha_h = 0.00029$, (d) $\beta_1 = 0.037$, $\Lambda = 9$, $\alpha_h = 0.00145$.

Time series behavior of system (2.1) for the symptomatic and asymptomatic population for the three Indian states and the whole country is depicted in Figure 10. We fix the parameters as in Figure 6, where the epidemic threshold is shown to be below unity for higher compliance of face masks of good quality. It is apparent from Figure 10 that if the face masks of higher quality are used in the public, then it will take almost three years to completely eradicate the disease from the nation. It is also evident from these plots that using face masks in public is very useful in minimizing community transmission and burden of COVID-19, provided their coverage level is high. Now, we see the combined effects of face masks and hospitalization of symptomatic individuals on the symptomatic population, Figure 11. The plots show that the symptomatic individuals completely disappear in a lesser time if the face masks of high quality are used together with hospitalization of confirmed infected individuals. Similarly, the combined effects of usage of face masks of higher quality and quarantine of asymptomatic individuals help to eradicate the asymptomatic infections in India, Figure 12. India is the third most affected country in the world by COVID-19. Almost all Indian states are affected by COVID-19 with leading cases in Maharastra, Tamil Nadu and Delhi. As currently no vaccine is available for the disease,

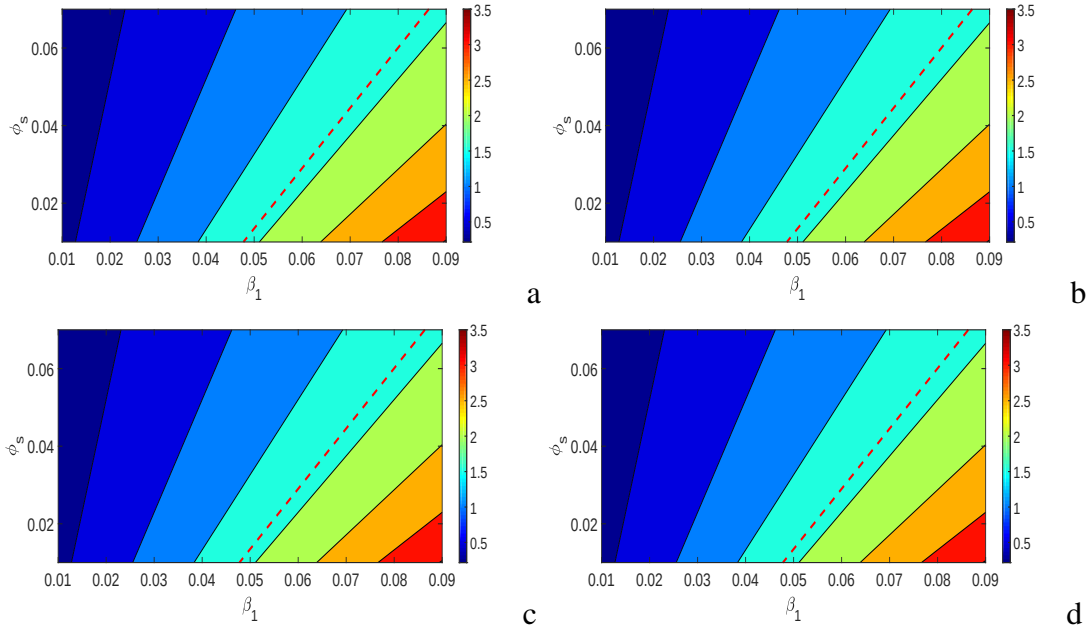


**Figure 7.** Contour plots of the basic reproduction number ($\mathcal{R}_0$) with respect $\beta_1$ and $\phi_s$ for (a) Maharashtra, (b) Delhi, (c) Tamil Nadu and (d) India. The dashed red line represents $\mathcal{R}_0 = 1$. Parameter values: $\beta_2 = 0.00003$, $\mu = 0.0042$, $\sigma = 0.000019$, $\mu_s = 0.06$, $\alpha_a = 0.0004$, $\gamma_a = 0.2$, $\gamma_h = 0.071$, $\mu_h = 0.05$, $a = 0.4$, $c_m = \epsilon_m = 0.99$; in (a) $\Lambda = 7$, $\alpha_h = 0.0019$, (b) $\Lambda = 9$, $\alpha_h = 0.0025$, (c) $\Lambda = 9$, $\alpha_h = 0.00029$, (d) $\Lambda = 9$, $\alpha_h = 0.00145$.

the ways of prevention include social distancing, using face masks, regular hand sanitization, proper lockdown. Imperfect lockdown in the country couldn't stop the rising number of cases. However, the pandemic can be effectively controlled or even eradicated if the masks-based intervention is combined with the hospitalization of symptomatic individuals and quarantine of asymptomatic individuals. In Figure 13, we have portrayed the global asymptotic stability of the endemic equilibrium $E_1$ in $I_s$–$I_a$–$H$ space. The figure depicts that all the solution trajectories originating from four different initial densities ultimately converge to the equilibrium $(I_s^*, I_a^*, H^*)$. The global asymptotic stability of the endemic equilibrium $E_1$ can also be extrapolated in other spaces.

## 5. Stochastic model

As all natural and man made systems are prone to stochastic perturbations. Here, we extend our deterministic model (2.1) to corresponding stochastic model. The motivation for the study of the stochastic model lies in the fact that when populations are small, the dynamics can be severely affected by small changes in the parameters. Thus, for initial phase of the disease outbreak, such as COVID-19, the stochastic model setup looks appropriate as at most of the places the infection is confined to small localities or geographic regions. Hence, a relevant and important information can be extracted from the stochastic model.

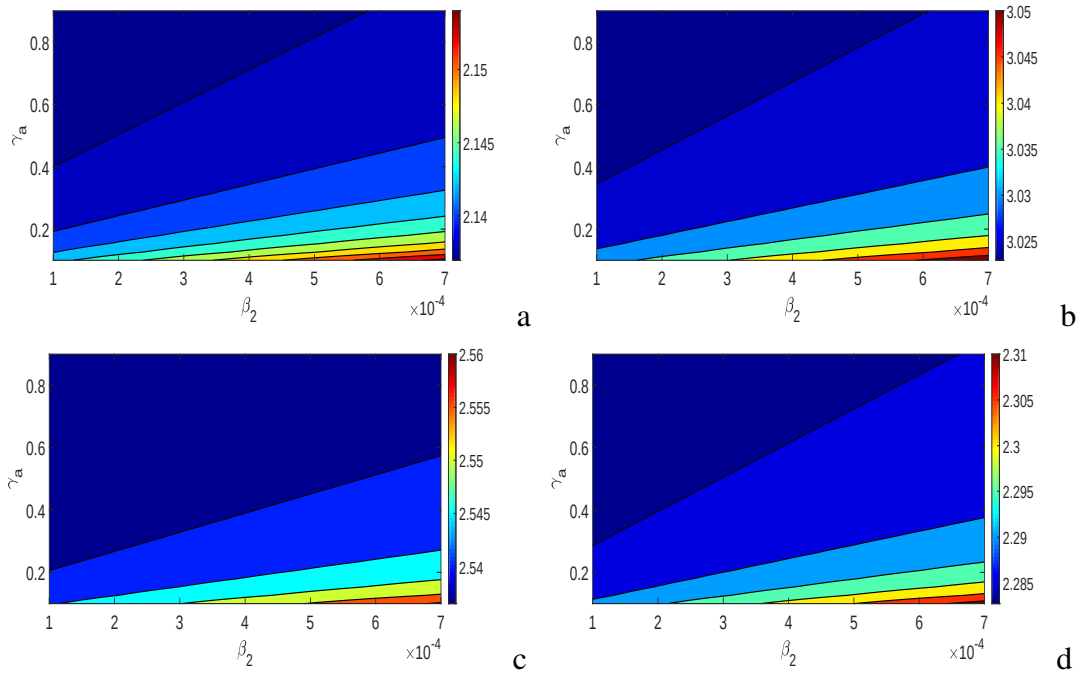


**Figure 8.** Contour plots of the basic reproduction number ($\mathcal{R}_0$) with respect $\beta_2$ and $\gamma_a$ for (a) Maharashtra, (b) Delhi, (c) Tamil Nadu and (d) India. Parameter values: $\mu = 0.0042$, $\sigma = 0.000019$, $\mu_s = 0.06$, $\alpha_a = 0.0004$, $\phi_s = 0.025$, $\gamma_h = 0.071$, $\mu_h = 0.05$, $a = 0.4$, $c_m = \epsilon_m = 0.99$; in (a) $\beta_1 = 0.065$, $\Lambda = 7$, $\alpha_h = 0.0019$, (b) $\beta_1 = 0.054$, $\Lambda = 9$, $\alpha_h = 0.0025$, (c) $\beta_1 = 0.049$, $\Lambda = 9$, $\alpha_h = 0.00029$, (d) $\beta_1 = 0.037$, $\Lambda = 9$, $\alpha_h = 0.00145$.

The derivation of an stochastic differential equation (SDE) model is based on the idea developed by Yuan et al. [36]. Let $X(t) = (X_1(t), X_2(t), X_3(t), X_4(t), X_5(t), X_6(t), X_7(t))^T$ be a continuous random variable for $(S(t), E(t), I_s(t), I_a(t), H(t), Q_h(t), R(t))^T$, where $T$ denotes the transpose of the matrix. Further, let $\Delta X = X(t + \Delta t) - X(t) = (\Delta X_1(t), \Delta X_2(t), \Delta X_3(t), \Delta X_4(t), \Delta X_5(t), \Delta X_6(t), \Delta X_7(t))^T$ denotes the random vector for the change in random variables during time interval $\Delta t$. Here, we will write the transition maps which define all possible changes between states in the SDE model. Based on our deterministic model (2.1), we see that there exist 19 possible changes between states in a small time interval $\Delta t$ (see Table 5). Here, it is emphasized that one and only one change is possible in the time $\Delta t$. For example, let us consider the case when one uninfected individual being infected by COVID-19. This will be given by the state change $\Delta X = (-1, 1, 0, 0, 0, 0, 0)$, and the change in its probability is given by

$$\begin{aligned}&\text{prob}(\Delta X_1, \Delta X_2, \Delta X_3, \Delta X_4, \Delta X_5, \Delta X_6, \Delta X_7)\\ &\quad = (-1, 1, 0, 0, 0, 0, 0)|(X_1, X_2, X_3, X_4, X_5, X_6, X_7) = P_1 = \beta X_1 X_2 \Delta t + O(\Delta t).\end{aligned}$$

One can easily determine the expectation change $E(\Delta X)$ and its covariance matrix $V(\Delta X)$ associated with $\Delta X$ by neglecting the terms higher than $O(\Delta t)$. The expectation of $\Delta X$ is given by

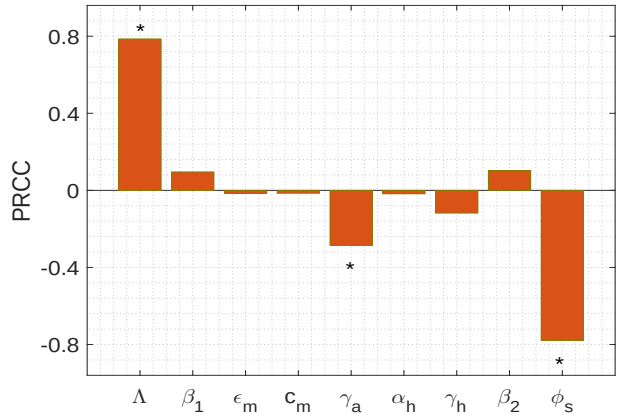


**Figure 9.** Effect of uncertainty of the model (2.1) on symptomatic infected population. Baseline values of parameters are chosen as $\beta_1 = 0.6$, $\beta_2 = 0.00053$, $\Lambda = 1000$, $\epsilon_m = 0.5$, $c_m = 0.1$, $\mu = 0.00004$, $\sigma = 0.19$, $\mu_s = 0.005$, $\alpha_a = 0.05$, $\alpha_h = 0.002$, $\gamma_a = 0.2$, $\phi_s = 0.025$, $\gamma_h = 0.071$, $\mu_h = 0.006$, $a = 0.3$. Significant parameters are marked by * (p-value< 0.05).

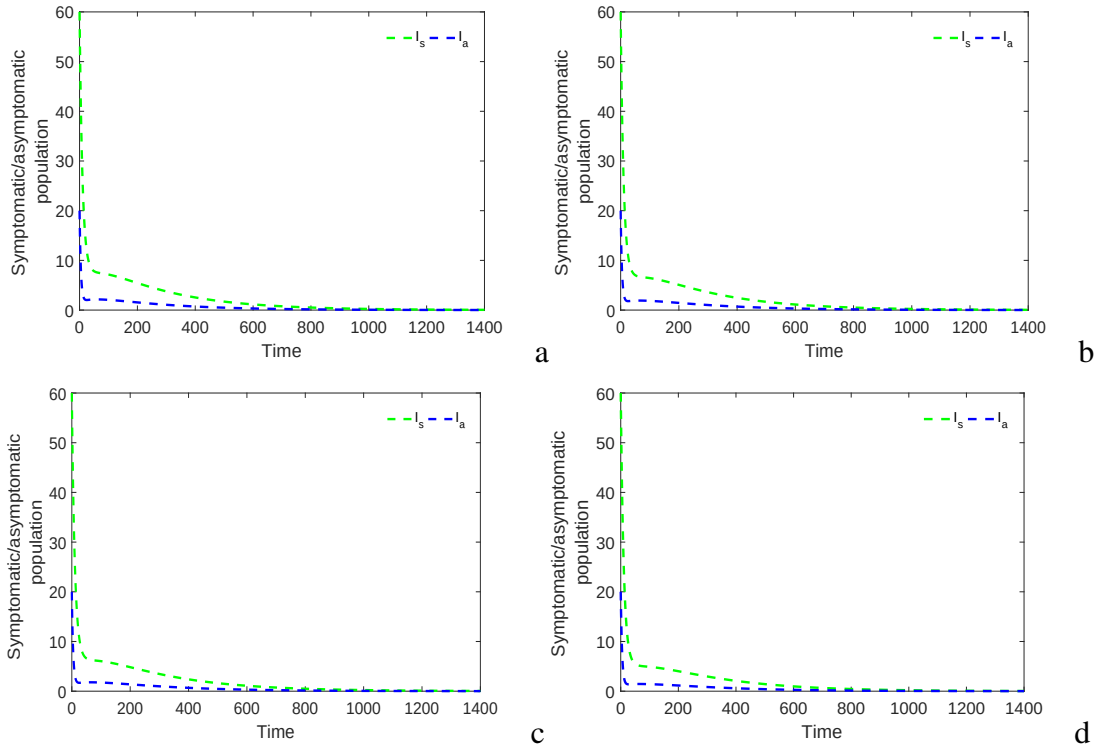


**Figure 10.** Time series of system (2.1) showing the impacts of high efficacy and compliance of face masks on the control of COVID-19 in (a) Maharashtra, (b) Delhi, (c) Tamil Nadu and (d) India. Parameters are at the same values as in Figure 6, and $\epsilon_m = c_m = 0.99$.

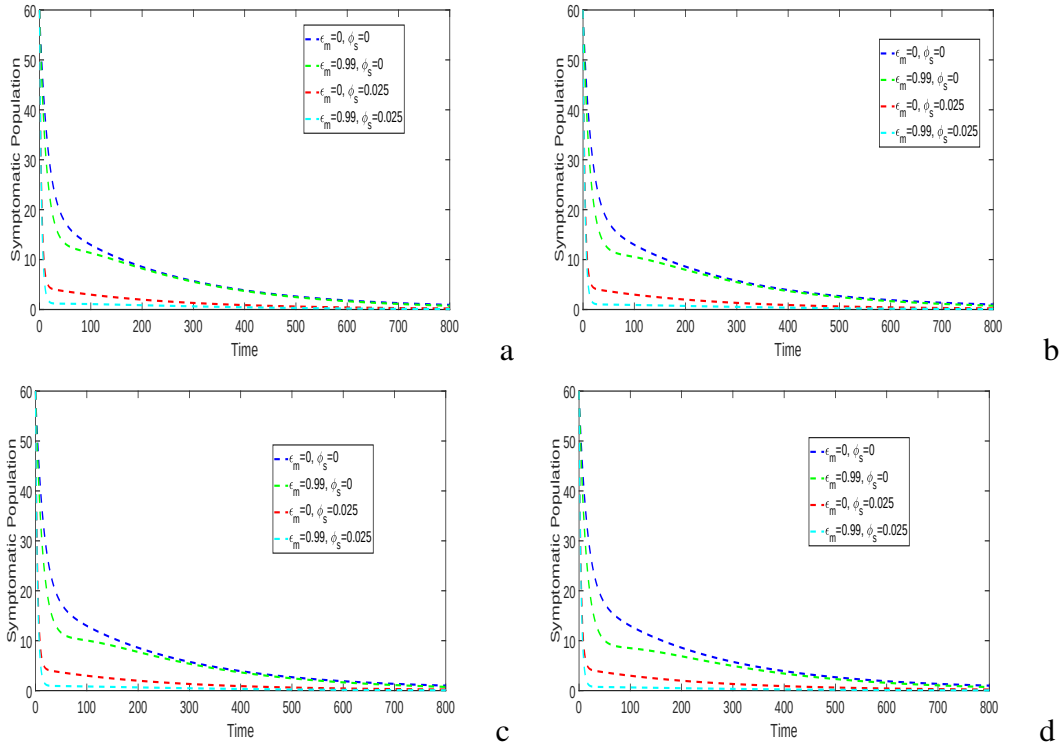


**Figure 11.** Time series of system (2.1) showing the impacts of efficacy of face masks and hospitalization of symptomatic individuals on the control of COVID-19 in (a) Maharashtra, (b) Delhi, (c) Tamil Nadu and (d) India. Rest of the parameters are at the same values as in Figure 6, and $c_m = 0.99$.

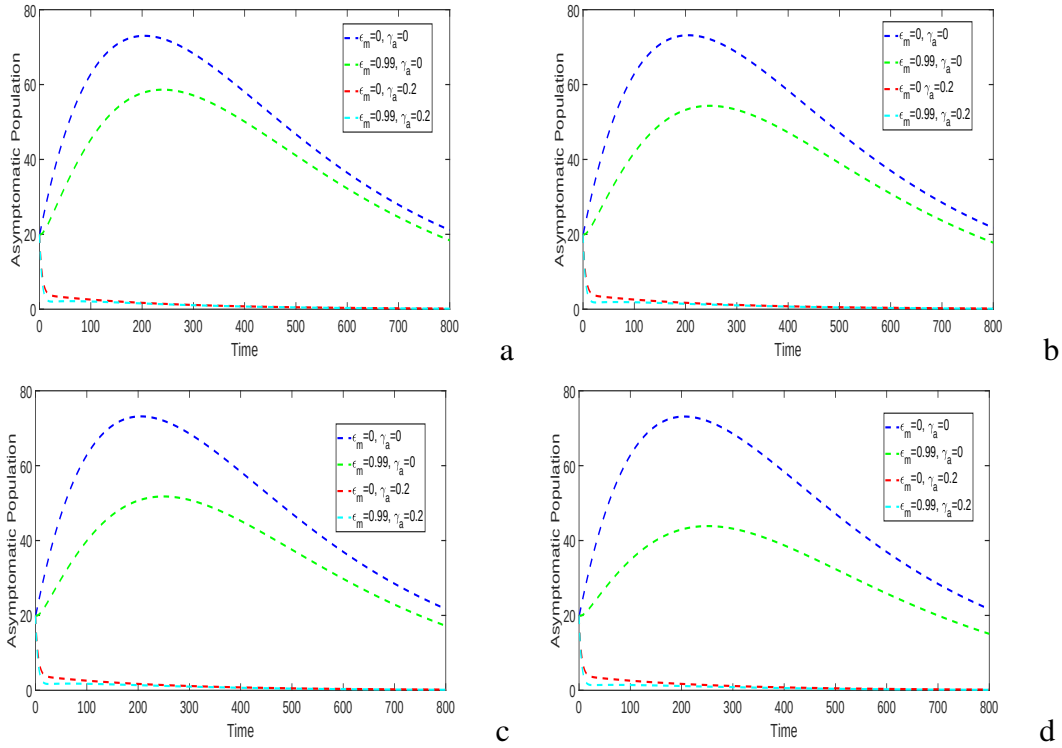


**Figure 12.** Time series of system (2.1) showing the impacts of efficacy of face masks and quarantine of asymptomatic individuals on the control of COVID-19 in (a) Maharashtra, (b) Delhi, (c) Tamil Nadu and (d) India. Rest of the parameters are at the same values as in Figure 6, and $c_m = 0.99$.

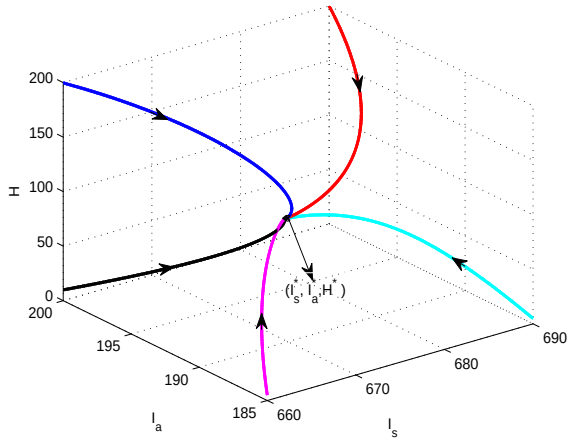


**Figure 13.** Global stability of the endemic equilibrium $E_1$ of system (2.1). Values of parameters are chosen as $\beta_1 = 0.037$, $\beta_2 = 0.05$, $\Lambda = 100$, $\epsilon_m = 0.005$, $c_m = 0.001$, $\mu = 0.0042$, $\sigma = 0.19$, $\mu_s = 0.06$, $\alpha_a = 0.004$, $\alpha_h = 0.145$, $\gamma_a = 0.2$, $\phi_s = 0.025$, $\gamma_h = 0.071$, $\mu_h = 0.05$, $a = 0.4$. Figure shows that solution trajectories starting from four different initial points ultimately converge to the components of equilibrium $E_1$.

$$
\begin{aligned}
E(\Delta X) &= \sum_{i=1}^{20} P_i(\Delta X)_i \Delta t \\
&= \begin{pmatrix}
\Lambda - \beta_1(1-\epsilon_m c_m)X_1X_3 - \beta_2(1-\epsilon_m c_m)X_1X_4 - \mu X_1 \\
\beta_1(1-\epsilon_m c_m)X_1X_3 - \beta_2(1-\epsilon_m c_m)X_1X_4 - (1-a)\sigma X_2 - a\sigma X_2 - \mu X_2 \\
(1-a)\sigma X_2 + \alpha_a X_4 - (\mu_s + \mu)X_3 - \phi_s X_3 \\
a\sigma X_2 - \gamma_a X_4 - \alpha_a X_4 - \mu X_4 \\
\phi_s X_3 - (\gamma_h + \mu_h + \mu)X_5 \\
\gamma_a X_4 - \alpha_h X_6 - \mu X_6 \\
\alpha_h X_6 + \gamma_h X_5 - \mu X_7
\end{pmatrix} \Delta t \\
&= f(X_1, X_2, X_3, X_4, X_5, X_6, X_7)\Delta t.
\end{aligned}
$$

Here, it can be noted that the expectation vector and the function $f$ are in the same form as those in deterministic system (2.1). Since the covariance matrix

$$V(\Delta X) = E((\Delta X)(\Delta X)^T) - E(\Delta X)E((\Delta X)^T),\ E(\Delta X)E((\Delta X)^T) = f(X)(f(X)^T).$$

An approximation of the covariance matrix of $\Delta X$ to order $\Delta t$ leads to product of the diffusion matrix ($\Omega$) and $\Delta t$. Thus, we get

$$
\begin{aligned}
E((\Delta X)(\Delta X)^T) &= \sum_{i=1}^{20} P_i((\Delta X)_i(\Delta X)_i^T)\Delta t \\
&= \begin{pmatrix}
V_{11} & V_{12} & 0 & 0 & 0 & 0 & 0 \\
0 & V_{22} & V_{23} & V_{24} & 0 & 0 & 0 \\
0 & V_{32} & V_{33} & V_{34} & V_{35} & 0 & 0 \\
0 & V_{42} & V_{43} & V_{44} & 0 & V_{46} & 0 \\
0 & 0 & V_{53} & 0 & V_{55} & 0 & V_{57} \\
0 & 0 & 0 & V_{64} & 0 & V_{66} & V_{67} \\
0 & 0 & 0 & 0 & V_{75} & V_{76} & V_{77}
\end{pmatrix} .\Delta t = \Omega.\Delta t,
\end{aligned}
$$

where

$$
\begin{aligned}
V_{11} &= P_1 + P_2 + P_3 + P_4 = \Lambda + \beta_1(1-\epsilon_m c_m)X_1X_3 + \beta_2(1-\epsilon_m c_m)X_1X_4 + \mu X_1, \\
V_{12} &= V_{21} = -P_2 - P_3 = -\beta_1(1-\epsilon_m c_m)X_1X_3 - \beta_2(1-\epsilon_m c_m)X_1X_4, \\
V_{22} &= P_2 + P_3 + P_5 + P_6 + P_7 \\
&= \beta_1(1-\epsilon_m c_m)X_1X_3 + \beta_2(1-\epsilon_m c_m)X_1X_4 + (1-a)\sigma X_2 + a\sigma X_2 + \mu X_2, \\
V_{23} &= V_{32} = -P_5 = -(1-a)\sigma X_2,\ V_{24} = V_{42} = -P_6 = -a\sigma X_2, \\
V_{33} &= P_5 + P_8 + P_9 + P_{10} + P_{11} = (1-a)\sigma X_2 + \alpha_a X_4 + \phi_s X_3 + \mu_s X_3 + \mu X_3, \\
V_{34} &= V_{43} = -P_8 = -\alpha_a X_4,\ V_{35} = V_{53} = -P_9 = -\phi_s X_3, \\
V_{44} &= P_6 + P_8 + P_{12} + P_{13} = a\sigma X_2 + \alpha_a X_4 + \gamma_a X_4 + \mu X_4, \\
V_{46} &= V_{64} = -P_{12} = -\gamma_a X_4,\ V_{55} = P_9 + P_{14} + P_{15} + P_{16} = \phi_s X_3 + \gamma_h X_5 + \mu X_5 + \mu_h X_5,
\end{aligned}
$$

$$
\begin{aligned}
V_{57} &= V_{75} = -P_{14} = -\gamma_h X_4,\ V_{66} = P_{12} + P_{17} + P_{19} = \gamma_a X_4 + \alpha_h X_6 + \mu X_6,\\
V_{66} &= P_{10} + P_{18} + P_{19} = \nu X_3 + \gamma X_6 + \mu X_7,\ V_{67} = V_{76} = -P_{17} = -\alpha_h X_6,\\
V_{77} &= P_{17} + P_{14} + P_{18} = \alpha_h X_6 + \gamma_h X_5 + \mu X_7.
\end{aligned}
$$

The diffusion matrix $\Omega$ is symmetric and positive definite.

Using the approach of [36], we construct a matrix $M$ such that $\Omega = MM^T$, where $M$ is a $7 \times 15$ matrix given as

$$
M = \begin{pmatrix}
M_1^1 & M_1^2 & 0 & 0 & 0 & 0 & 0 & 0 & 0 & 0 & 0 & 0 & 0 & 0 & 0\\
0 & M_2^2 & M_2^3 & M_2^4 & M_2^5 & 0 & 0 & 0 & 0 & 0 & 0 & 0 & 0 & 0 & 0\\
0 & 0 & 0 & M_3^4 & 0 & M_3^6 & M_3^7 & M_3^8 & M_3^9 & 0 & 0 & 0 & 0 & 0 & 0\\
0 & 0 & 0 & 0 & M_4^5 & 0 & M_4^7 & 0 & M_4^9 & M_4^{10} & 0 & 0 & 0 & 0 & 0\\
0 & 0 & 0 & 0 & 0 & 0 & 0 & M_5^8 & 0 & 0 & M_5^{11} & M_5^{12} & 0 & 0 & 0\\
0 & 0 & 0 & 0 & 0 & 0 & 0 & 0 & 0 & M_6^{10} & 0 & 0 & M_6^{13} & M_6^{14} & 0\\
0 & 0 & 0 & 0 & 0 & 0 & 0 & 0 & 0 & 0 & 0 & M_7^{12} & 0 & M_7^{14} & M_7^{15}
\end{pmatrix},
$$

where

$$
\begin{aligned}
&M_1^1 = \sqrt{P_1 + P_4}, M_1^2 = \sqrt{P_2 + P_3}, M_2^2 = -\sqrt{P_2 + P_3}, M_2^3 = \sqrt{P_7}, M_2^4 = \sqrt{P_5}, M_2^5 = \sqrt{P_6},\\
&M_3^4 = -\sqrt{P_5}, M_3^6 = -\sqrt{P_{10} + P_{11}}, M_3^7 = \sqrt{P_8}, M_3^8 = \sqrt{P_9}, M_4^5 = -\sqrt{P_6}, M_4^7 = -\sqrt{P_8},\\
&M_4^9 = \sqrt{P_{13}}, M_4^{10} = \sqrt{P_{12}}, M_5^8 = -\sqrt{P_9}, M_5^{11} = \sqrt{P_{15} + P_{16}}, M_5^{12} = \sqrt{P_{14}}, M_6^{10} = -\sqrt{P_{12}},\\
&M_6^{13} = \sqrt{P_{19}}, M_6^{14} = \sqrt{P_{17}}, M_7^{12} = -\sqrt{P_{14}}, M_7^{14} = -\sqrt{P_{17}}, M_7^{15} = \sqrt{P_{18}}.
\end{aligned}
$$

Then, Ito stochastic differential model has the form,

$$
d(X(t)) = f(X_1, X_2, X_3, X_4, X_5, X_6, X_7)dt + M.dW(t)
$$

with initial condition

$$
X(0) = (X_1(0), X_2(0), X_3(0), X_4(0), X_5(0), X_6(0), X_7(0))^T
$$

and a Wiener process,

$$
\begin{aligned}
W(t) = (&W_1(t), W_2(t), W_3(t), W_4(t), W_5(t), W_6(t), W_7(t), W_8(t), W_9(t), W_{10}(t), W_{11}(t), W_{12}(t),\\
&W_{13}(t), W_{14}(t), W_{15}(t))^T.
\end{aligned}
$$

In view of the above facts, we construct the stochastic differential equation model as,

$$
\begin{aligned}
dS &= (\Lambda - \beta_1(1-\epsilon_m c_m)SI_s - \beta_2(1-\epsilon_m c_m)SI_a - \mu S)dt + \sqrt{\Lambda + \mu S}\,dW_1\\
&\quad + \sqrt{\beta_1(1-\epsilon_m c_m)SI_s + \beta_2(1-\epsilon_m c_m)SI_a}\,dW_2,\\
dE &= [\beta_1(1-\epsilon_m c_m)SI_s + \beta_2(1-\epsilon_m c_m)SI_a - \sigma E - \mu E]dt\\
&\quad - \sqrt{\beta_1(1-\epsilon_m c_m)SI_s + \beta_2(1-\epsilon_m c_m)SI_a}\,dW_2 + \sqrt{\mu E}\,dW_3 + \sqrt{(1-a)\sigma E}\,dW_4 + \sqrt{a\sigma E}\,dW_5,\\
dI_s &= [(1-a)\sigma E + \alpha_a I_a - (\mu_s + \mu)I_s - \phi_s I_s]dt - \sqrt{(1-a)\sigma E}\,dW_4 + \sqrt{(\mu_s + \mu)I_s}\,dW_6\\
&\quad + \sqrt{\alpha_a I_a}\,dW_7 + \sqrt{\phi_s I_s}\,dW_8,
\end{aligned}
$$

$$
\begin{aligned}
dI_a &= [a\sigma E - \gamma_a I_a - \alpha_a I_a - \mu I_a]dt - \sqrt{a\sigma E}dW_5 - \sqrt{\alpha_a I_a}dW_7 + \sqrt{\gamma_a I_a}dW_9 + \sqrt{\mu I_a}dW_{10}, \quad (5.1)\\
dH &= [\phi_s I_s - (\gamma_h + \mu_h + \mu)H]dt - \sqrt{\phi_s I_s}dW_8 + \sqrt{(\mu_h + \mu)H}dW_{11} + \sqrt{\gamma_h H}dW_{12},\\
dQ_h &= [\gamma_a I_a - \alpha_h Q_h - \mu Q_h]dt - \sqrt{\gamma_a I_a}dW_9 + \sqrt{\mu Q_h}dW_{13} + \sqrt{\alpha_h Q_h}dW_{14},\\
dR &= [\alpha_h Q_h + \gamma_h H - \mu R]dt - \sqrt{\gamma_h H}dW_{12} - \sqrt{\alpha_h Q_h}dW_{14} + \sqrt{\mu R}dW_{15}.
\end{aligned}
$$

### *5.1. Stochastic simulation results*

To emphasise the impact of stochasticity in the model system, we simulate the stochastic model (5.1) by using Euler-Maruyama method [36]. For this purpose, we use the following set of parameter values:

$$
\begin{aligned}
&\beta_1 = 0.03,\ \beta_2 = 0.00003,\ \Lambda = 10,\ \epsilon_m = 0.5,\ c_m = 0.1,\ \mu = 0.000042,\ \sigma = 0.19,\ \mu_s = 0.06,\\
&\alpha_a = 0.01,\ \alpha_h = 0.0002,\ \gamma_a = 0.02,\ \phi_s = 0.025,\ \gamma_h = 0.071,\ \mu_h = 0.05,\ a = 0.4. \quad (5.2)
\end{aligned}
$$

We perform simulations of system (5.1) for 120 days and 100 simulation runs fixing $\Delta t = 0.5$. First, we compare the mean of 100 runs of stochastic model simulation with the results of corresponding deterministic model, and plot time series of all the variables (see Figure 14). From the figures, it can be inferred that the mean of 100 runs of stochastic simulation is very close to the simulation results of deterministic model for the susceptible population ($S$) whereas for other populations, a little bit deviations between stochastic and deterministic simulations results are apparent. To further see the impact of stochasticity on infective population, we plot the 100 simulation runs of the symptomatic ($I_s$) and asymptomatic ($I_a$) infected populations in Figure 15. It may be noted that due to presence of noise, the $I_s$ and $I_a$ populations do not approach to their respective equilibrium components $I_s^*$ and $I_a^*$; rather they are distributed near the equilibrium values.

In order to understand these results better, we also plot the distributions of both the populations at 80th, 100th and 120th days. The results for distribution of symptomatic infected population ($I_s$) are provided in Figure 16. One can easily see the change in distribution of the population as time progresses. Importantly, we note that the distribution of trajectories become close to range 85-90 at 120th day from more distributed range 75–90 on 80th day. Thus, the trajectories become more concentrated around 85–90 with passage of time. In Figure 17, we plot the distribution of asymptomatic infected population ($I_s$). It may be noted from the figure that the distribution of trajectories clearly shift from left to right of 120 level and on day 120 they concentrate in range 120–130. These distributions of $I_s$ and $I_a$ provide insightful information about the behaviors of trajectories when the system is allowed to have stochastic influence.

## 6. Conclusion and discussion

COVID-19 is now one of the deadliest pandemic in human history and has had tragic consequences affecting millions of people worldwide. In India, the outbreak of COVID-19 started on 2nd March 2020 and after that, the cases are on an ever-increasing trajectory. With very high population density, the unavailability of specific medication or vaccine and insufficient information about the transmission mechanism of the disease makes it extremely difficult to fight against the disease effectively. Designing an efficient control strategy is one of the crucial factors to curb the disease spread in an outbreak

**Table 5.** Possible changes of states and their probabilities.

| Possible state change | Probability of state change |
|---|---|
| $(\Delta X)_1 = (1,0,0,0,0,0,0)^T$ | $P_1 = \Lambda\Delta t + O(\Delta t)$ |
| Rate of recruitment in human population | |
| $(\Delta X)_2 = (-1,1,0,0,0,0,0)^T$ | $P_2 = \beta_1(1-\epsilon_m c_m)X_1X_3\Delta t + O(\Delta t)$ |
| Change when people meet symptomatic infective ($I_s$) | |
| and become exposed | |
| $(\Delta X)_2 = (-1,1,0,0,0,0,0)^T$ | $P_3 = \beta_1(1-\epsilon_m c_m)X_1X_4\Delta t + O(\Delta t)$ |
| Change when people meet asymptomatic infective ($I_a$) | |
| and become exposed | |
| $(\Delta X)_4 = (-1,0,0,0,0,0,0)^T$ | $P_4 = \mu X_1\Delta t + O(\Delta t)$ |
| Natural death rate of susceptible population | |
| $(\Delta X)_5 = (0,-1,1,0,0,0,0)^T$ | $P_5 = (1-a)\sigma X_2\Delta t + O(\Delta t)$ |
| Change when fraction of exposed people move | |
| to symptomatic infected class ($I_s$) | |
| $(\Delta X)_6 = (0,-1,0,1,0,0,0)^T$ | $P_6 = a\sigma X_2\Delta t + O(\Delta t)$ |
| Change when fraction of exposed people move | |
| to asymptomatic infected class ($I_a$) | |
| $(\Delta X)_7 = (0-1,0,0,0,0,0,0)^T$ | $P_7 = \mu X_2\Delta t + O(\Delta t)$ |
| Natural death rate of exposed population | |
| $(\Delta X)_8 = (0,0,1,-1,0,0,0)^T$ | $P_8 = \alpha_a X_4\Delta t + O(\Delta t)$ |
| Change when asymptomatic population join symptomatic class | |
| $(\Delta X)_9 = (0,0,-1,0,1,0,0)^T$ | $P_9 = \phi_s X_3\Delta t + O(\Delta t)$ |
| Change when symptomatic people move to hospitalized class | |
| $(\Delta X)_{10} = (0,0,-1,0,0,0,0)^T$ | $P_{10} = \mu_s X_3\Delta t + O(\Delta t)$ |
| Disease related death rate of symptomatic population | |
| $(\Delta X)_{11} = (0,0,-1,0,0,0,0)^T$ | $P_{11} = \mu X_3\Delta t + O(\Delta t)$ |
| Natural death rate of symptomatic population | |
| $(\Delta X)_{12} = (0,0,0,-1,0,1,0)^T$ | $P_{12} = \gamma_a X_4\Delta t + O(\Delta t)$ |
| Change when asymptomatic people move to home quarantined class | |
| $(\Delta X)_{13} = (0,0,0,-1,0,0,0)^T$ | $P_{13} = \mu X_4\Delta t + O(\Delta t)$ |
| Natural death rate of asymptomatic population | |
| $(\Delta X)_{14} = (0,0,0,0,-1,0,1)^T$ | $P_{14} = \gamma_h X_5\Delta t + O(\Delta t)$ |
| Change when hospitalized infected with COVID-19 will join the recovered class | |
| $(\Delta X)_{15} = (0,0,0,0,-1,0,0)^T$ | $P_{15} = \nu X_3\Delta t + O(\Delta t)$ |
| Natural death rate of hospitalized population | |
| $(\Delta X)_{16} = (0,0,0,0,-1,0,0)^T$ | $P_{11} = \mu X_3\Delta t + O(\Delta t)$ |
| Disease related death rate of hospitalized people with COVID-19 | |
| $(\Delta X)_{17} = (0,0,0,0,0,-1,1)^T$ | $P_{17} = \alpha_h X_6\Delta t + O(\Delta t)$ |
| Change when self-quarantined people will join the recovered class | |
| $(\Delta X)_{18} = (0,0,0,0,0,0,-1)^T$ | $P_{18} = \mu X_7\Delta t + O(\Delta t)$ |
| Natural death rate of recovered individuals | |
| $(\Delta X)_{19} = (0,0,0,0,0,-1,0)^T$ | $P_{19} = \mu X_6\Delta t + O(\Delta t)$ |
| Natural death rate of self-quarantined individuals | |
| $(\Delta X)_{20} = (0,0,0,0,0,0,0,0,0)^T$ | $P_{20} = 1 - \sum_{i=1}^{19} P_i\Delta t + O(\Delta t)$ |
| No change | |

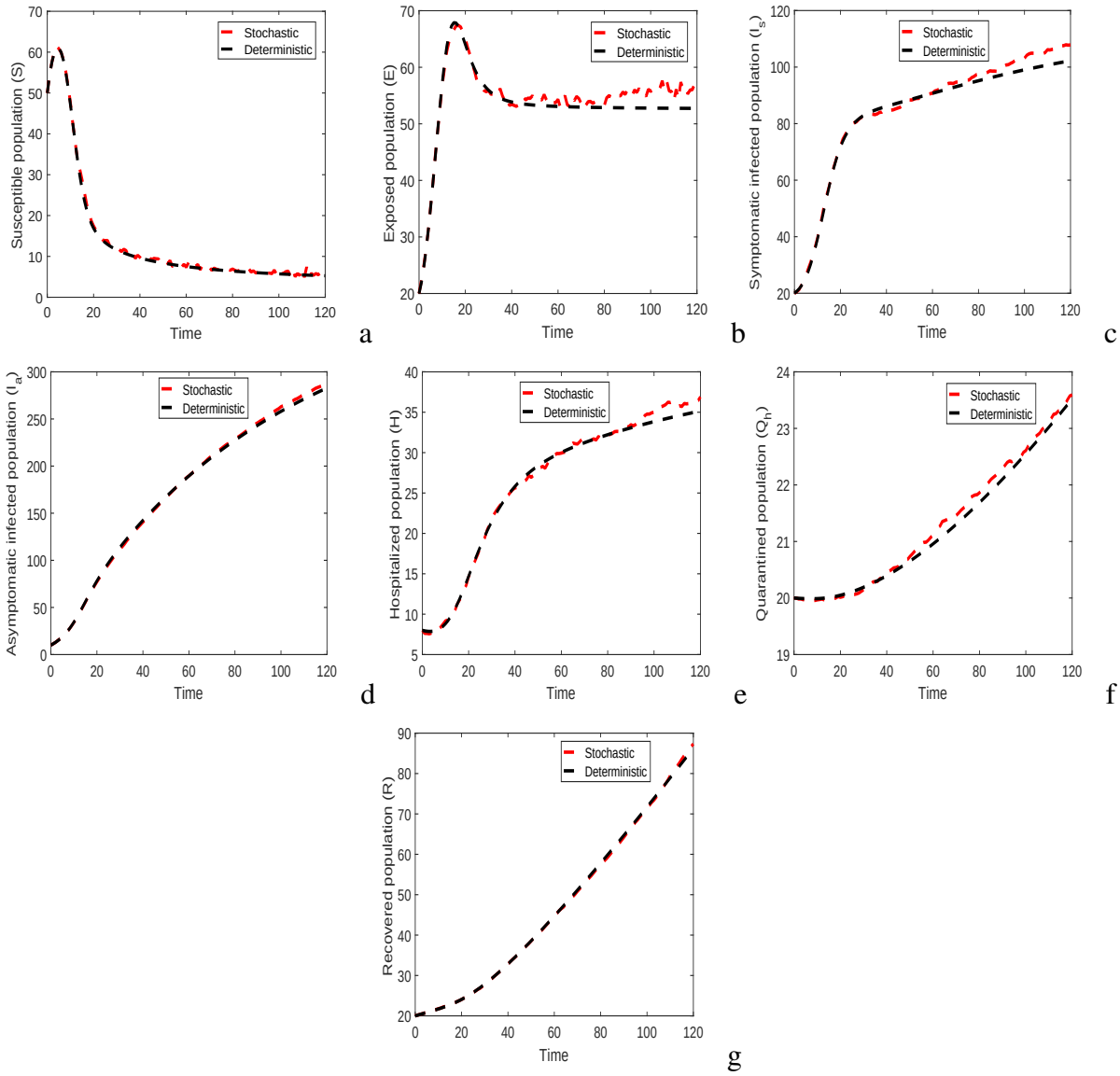


**Figure 14.** Time evolutions of (a) $S$, (b) $E$, (c) $I_s$, (d) $I_a$, (e) $H$, (f) $Q_h$ and (g) $R$ for deterministic and stochastic systems.

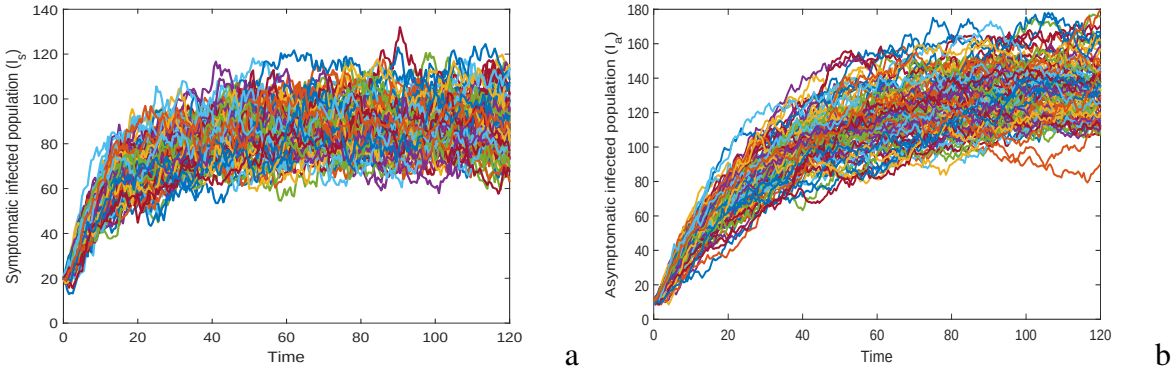


**Figure 15.** Trajectories of (a) symptomatic ($I_s$) and (b) asymptomatic ($I_a$) infected populations for 100 simulation runs.

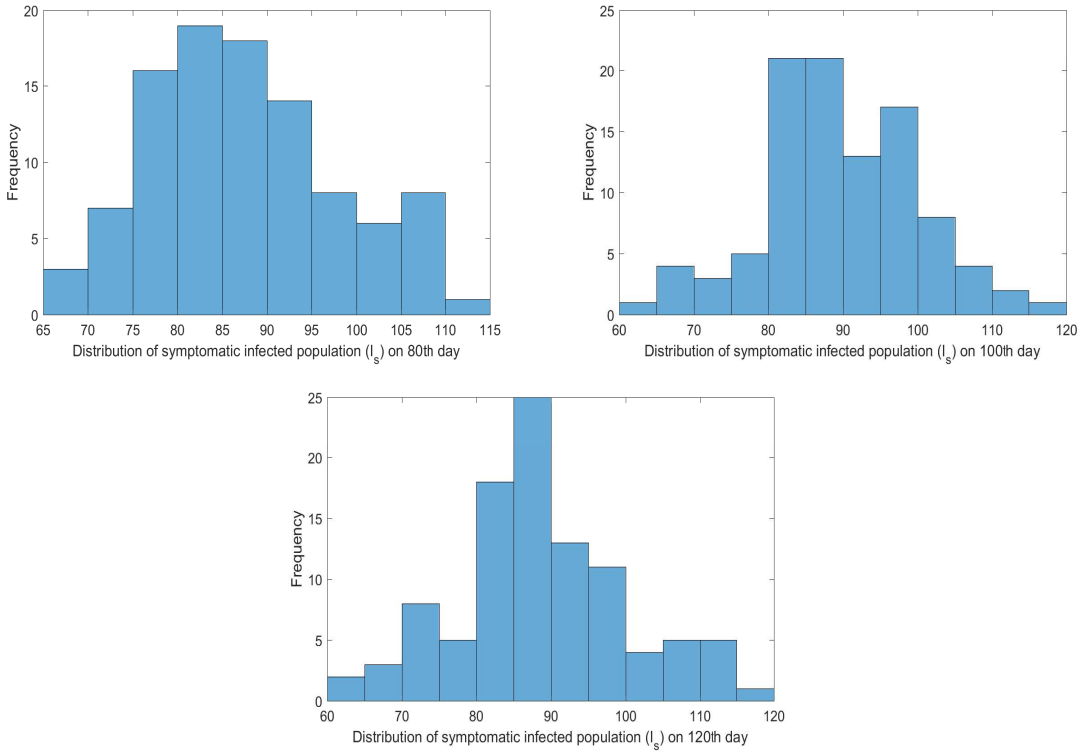


**Figure 16.** Distributions of symptomatic infected population ($I_s$) on days 80, 100 and 120.

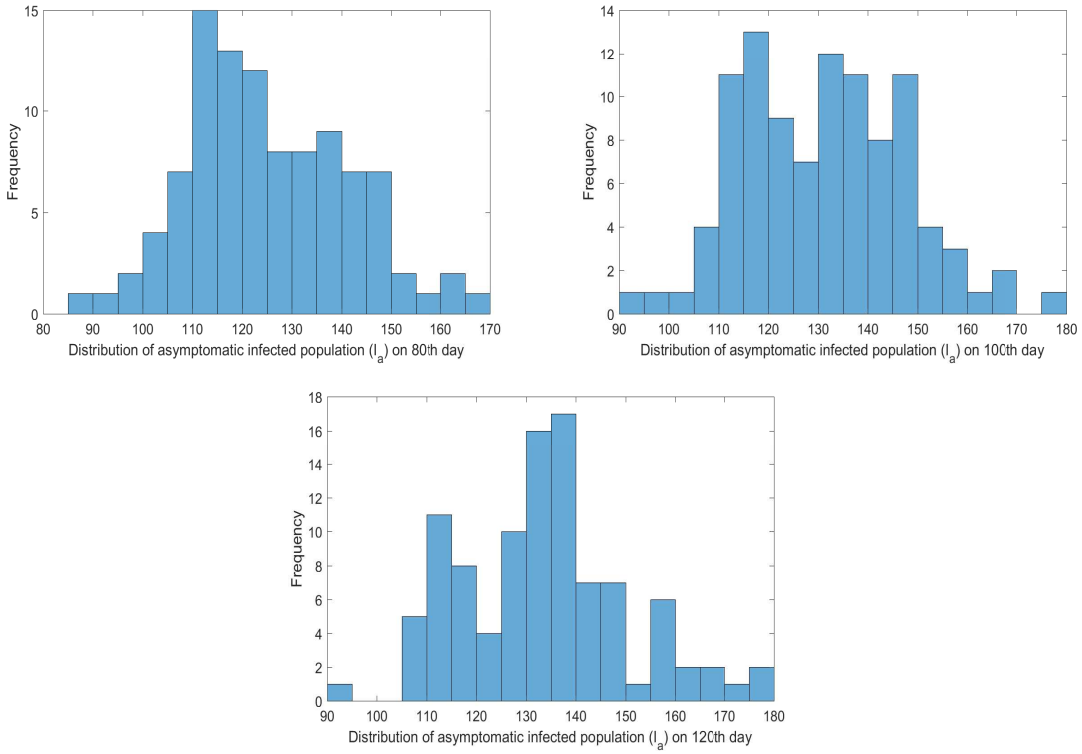


**Figure 17.** Distributions of asymptomatic infected population ($I_a$) on days 60, 80 and 100.

situation. In this study, we first proposed a deterministic compartmental model to describe the disease transmission mechanism in the population. Our first goal was to incorporate the effect of asymptomatic infective on the dynamics of the disease whereas another aim was to see the impacts of the proper use of face masks, hospitalization of symptomatic individuals and quarantine of asymptomatic individuals on the disease control. Our study focusses on the outbreak of COVID-19 in India and hence we have used the four data sets consisting of three states of the high incidences of COVID-19 in India (Maharashtra, Delhi and Tamil Nadu) and overall country data. These data sets are for the cumulative active cases of the disease. The purpose of selecting the active cases is inspired by the fact that this data is real representative of the actual disease load and also reflects the need for preparedness from the public health and policymakers. Our proposed model is then fitted to these data sets and we estimated the transmission rate of disease between symptomatic individuals and susceptibles, and the recovery rate of quarantined individuals. By looking at the estimated parameters, it is observed that the rate of disease transmission is quite high in Maharastra which basically implies the high infectiousness of the disease. Based on the estimated parameters and actual COVID-19 incidence data, we estimated the basic reproduction number to get an overview of this phase of the outbreak. This suggests that the rate of disease transmission needs to be controlled otherwise a large proportion will be affected within a very short period of time. Our study also underlines short term predictions for the three states and India. It is concluded that the infective population will be on increasing curve for Maharashtra and India whereas we can see the settling of active cases for Tamil Nadu and Delhi. Sophisticated techniques of sensitivity analysis are employed to determine the impacts of model parameters on the basic reproduction number and symptomatic infected individuals.

Further, a comprehensive analysis of the impact of parameters associated with the interventions (use of face masks, hospitalizations of symptomatic individuals and quarantine of asymptomatic individuals) is performed numerically. Our results suggest that higher intervention efforts are needed to control the disease outbreak within a shorter period of time in India. Our analysis also reveals that the strength of the interventions should be increased over time to eradicate the disease effectively. Although the use of face masks in the public can significantly reduce COVID-19 in India, its use as a sole intervention strategy may fail to lead to the realistic elimination of the disease, as such elimination requires unrealistic high compliance in face masks usage in the public. COVID-19 elimination is feasible in India if the public face masks use strategy (using the masks with moderate efficacy, and moderate compliance in its usage) is complemented with hospitalization of symptomatic individuals and quarantine of asymptomatic individuals. Similar impact of face masks on the control of COVID-19 in Nigeria was observed by Iboi et al. [14]. COVID-19 can be effectively controlled using social-distancing measures provided its effectiveness level is at least moderate. The lockdown measures implemented in India on March 25, 2020, need to be maintained for effective containment of COVID-19 outbreaks in the country. Relaxing, or fully lifting, the lockdown measures sooner, in an effort to re-open the economy or the country, may trigger a deadly wave of the pandemic.

We also analyzed our model for the stability of the equilibrium points, and the corresponding results indicate that disease can be eradicated if the basic reproduction number is below unity that can be maintained by proper use of face masks of high quality. Motivated by the fact that when populations are small, the dynamics can be severely affected by small changes in the parameters, the deterministic model is extended to its stochastic counterpart. A numerical simulation is provided for the stochastic model. It is noted that the solution trajectories of the populations do not approach their equilibrium levels, rather, these trajectories are distributed near the equilibrium values. The distributions of symptomatic and asymptomatic infected populations are provided to show the behaviors of trajectories when the model system is affected by stochastic perturbations.

## Acknowledgements

The authors thank the associate editor and anonymous reviewers for valuable comments, which contributed to the improvement in the presentation of the paper. Pankaj Kumar Tiwari is thankful to University Grants Commissions, New Delhi, India for providing financial support in form of D.S. Kothari post-doctoral fellowship (No.F.4-2/2006 (BSR)/MA/17-18/0021). Mini Ghosh is supported by the research grants of DST, Govt. of India, via a sponsored research project: File No. MSC/2020/000051. The work of Yun Kang is partially supported by NSF-DMS (1313312 & 1716802); NSF-IOS/DMS (1558127), DARPA (ASC-SIM II), and The James S. McDonnell Foundation 21st Century Science Initiative in Studying Complex Systems Scholar Award (UHC Scholar Award 220020472).

## Conflict of interest

The authors declare that there is no conflict of interest in this paper.

## References


1. N. M. Ferguson, D. Laydon, G. Nedjati-Gilani, N. Imai, K. Ainslie, M. Baguelin, et al., Impact of non-pharmaceutical interventions (NPIs) to reduce COVID-19 mortality and healthcare demand, London: Imperial College COVID-19 Response Team, March 16, 2020.
2. M. McKee, D. Stuckler, If the world fails to protect the economy, COVID-19 will damage health not just now but also in the future, *Nat. Med.*, **26** (2020), 640–642.
3. M. Nicola, Z. Alsafi, C. Sohrabi, A. Kerwan, A. Al-Jabir, C. Iosifidis, et al., The socio-economic implications of the coronavirus pandemic (COVID-19): A review, *Int. J. Surg.*, **78** (2020), 185–193.
4. N. van Doremalen, T. Bushmaker, D. H. Morris, M. G. Holbrook, A. Gamble, B. N. Williamson, et al., Aerosol and surface stability of SARS-CoV-2 as compared with SARS-CoV-1, *N. Engl. J. Med.*, **382** (2020), 1564–1567.
5. World Health Organization, Coronavirus disease 2019 (COVID-19). WHO situation report - 73, 2020. Avaiable from: `https://www.who.int/docs/default-source/coronaviruse/situation-reports/20200402-sitrep-73-covid-19.pdf`.
6. X. Liu, S. Zhang, COVID-19: face masks and human-to-human transmission. Influenza Other Respir Viruses, 2020. Avaiable from: `http://doi.wiley.com/10.1111/irv.12740`.
7. C. J. Noakes, C. B. Beggs, P. A. Sleigh, K. G. Kerr, Modelling the transmission of airborne infections in enclosed spaces, *Epidemiol. Infect.*, **134** (2006), 1082–1091.
8. C. J. Noakes, P. A. Sleigh, Mathematical models for assessing the role of airflow on the risk of airborne infection in hospital wards, *J. R. Soc. Interface*, **6** (2009), S791–S800.
9. R. Chetty, M. Stepner, S. Abraham, S. Lin, B. Scuderi, N. Turner, et al., The association between income and life expectancy in the United States, 2001–2014, *JAMA*, **315** (2016), 1750.
10. R. O. Stutt, R. Retkute, M. Bradley, C. A. Gilligan, J. Colvin, A modelling framework to assess the likely effectiveness of facemasks in combination with 'lock-down'in managing the COVID-19 pandemic, *Proc. R. Soc. A*, **476** (2020), 20200376.
11. D. K. Chu, E. A. Akl, S. Duda, K. Solo, S. Yaacoub, H. J. Schunemann, et al., Physical distancing, face masks, and eye protection to prevent person-to-person transmission of SARS-CoV-2 and COVID-19: a systematic review and meta-analysis, *The Lancet*, **395** (2020), 1973–1987.
12. C. N. Ngonghala, E. Iboi, S. Eikenberry, M. Scotch, C. R. MacIntyre, M. H. Bonds, et al., Mathematical assessment of the impact of non-pharmaceutical interventions on curtailing the 2019 novel Coronavirus, *Math. Biosci.*, **325** (2020), 108364.
13. S. E. Eikenberry, M. Mancuso, E. Iboi, T. Phan, K. Eikenberry, Y. Kuang, et al., To mask or not to mask: Modeling the potential for face mask use by the general public to curtail the COVID-19 pandemic, *Infect. Dis. Model.*, **5** (2020), 293–308.
14. E. A. Iboi, O. O. Sharomi, C. N. Ngonghala, A. B. Gumel, Mathematical modeling and analysis of COVID-19 pandemic in Nigeria, *Math. Biosci. Eng.*, **17** (2020), 7192–7220.
15. D. Okuonghae, A. Omame, Analysis of a mathematical model for COVID-19 population dynamics in Lagos, Nigeria, *Chaos Soliton. Fract.*, **139** (2020), 110032.

16. B. J. Cowling, K. H. Chan, V. J. Fang, C. K. Cheng, R. O. Fung, W. Wai, et al., Facemasks and hand hygiene to prevent influenza transmission in households: a cluster randomized trial, *Ann. Intern. Med.*, **151** (2009), 437–446.
17. M. Lipsitch, T. Cohen, B. Cooper, J. M. Robins, S. Ma, L. James, et al., Transmission dynamics and control of severe acute respiratory syndrome, *Science*, **300** (2003), 1966–1970.
18. S. Zhao, L. Stone, D. Gao, S. S. Musa, M. K. Chong, D. He, et al., Imitation dynamics in the mitigation of the novel coronavirus disease (COVID-19) outbreak in Wuhan, China from 2019 to 2020, *Ann. Transl. Med.*, **8** (2020), 448.
19. S. H. A. Khoshnaw, R. H. Salih, S. Sulaimany, Mathematical modeling for coronavirus disease (COVID-19) in predicting future behaviours and sensitivity analysis, *Math. Model. Nat. Phenom.*, **15** (2020), 1–13.
20. M. Serhani, H. Labbardi, Mathematical modeling of COVID-19 spreading with asymptomatic infected and interacting peoples, *J. Appl. Math. Comput.*, **17** (2020), 1–20.
21. C. Huang, Y. Wang, X. Li, L. Ren, J. Zhao, Y. Hu, et al., Clinical features of patients infected with 2019 novel coronavirus in Wuhan, China, *Lancet*, **395** (2020), 497–506.
22. P. van den Driessche, J. Watmough, Reproduction numbers and sub-threshold endemic equilibria for compartmental models of disease transmission, *Math. Biosci.*, **180** (2002), 29–48.
23. COVID 2019, India, available from: `https://www.covid19india.org/`.
24. L. F. White, M. Pagano, A likelihood-based method for real-time estimation of the serial interval and reproductive number of an epidemic, *Stat. Med.*, **27** (2008), 2999–3016.
25. A. Davies, K. A. Thompson, K. Giri, G. Kafatos, J. Walker, A. Bennett, Testing the efficacy of homemade masks: would they protect in an influenza pandemic?, *Disaster Med. Public Health Prep.*, **7** (2013), 413–418.
26. C. N. Ngonghala, E. Iboi, S. Eikenberry, M. Scotch, C. R. MacIntyre, M. H. Bonds, et al., Mathematical assessment of the impact of non-pharmaceutical interventions on curtailing the 2019 novel coronavirus, *Math. Biosci.*, **325** (2020), 108364.
27. S. A. Lauer, K. H. Grantz, Q. Bi, F. K. Jones, Q. Zheng, H. R. Meredith, et al., The incubation period of coronavirus disease 2019 (COVID-19) from publicly reported confirmed cases: estimation and application, *Ann. Intern. Med.*, **172** (2020), 577–582.
28. R. Li, S. Pei, B. Chen, Y. Song, T. Zhang, W. Yang, et al., Substantial undocumented infection facilitates the rapid dissemination of novel coronavirus (SARS-CoV2), *Science*, **368** (2020), 489–493.
29. F. Zhou, T. Yu, R. Du, G. Fan, Y. Liu, Z. Liu, et al., Clinical course and risk factors for mortality of adult inpatients with COVID-19 in Wuhan, China: a retrospective cohort study, *Lancet*, **395** (2020), 1054–1062.
30. B. Tang, X. Wang, Q. Li, N. L. Bragazzi, S. Tang, Y. Xiao, et al., Estimation of the transmission risk of the 2019-nCoV and its implication for public health interventions, *J. Clin. Med.*, **9** (2020), 462.
31. D. Aldila, M. Z. Ndii, B. M. Samiadji, Optimal control on COVID-19 eradication program in Indonesia under the effect of community awareness, *Math. Biosci. Eng.*, **17** (2020), 6355–6389.

32. D. He, S. Zhao, X. Xu, Q. Lin, Z. Zhuang, P. Cao, et al., Low dispersion in the infectiousness of COVID-19 cases implies difficulty in control, *BMC Public Health*, **20** (2020), 1558.

33. I. Ghosh, P. K. Tiwari, J. Chattopadhyay, Effect of active case finding on dengue control: Implications from a mathematical model, *J. Theor. Biol.*, **464** (2019), 50–62.

34. S. M. Blower, H. Dowlatabadi, Sensitivity and uncertainty analysis of complex models of disease transmission: an HIV model, as an example, *Int. Stat. Rev.*, **62** (1994), 229–243.

35. S. Marino, I. B. Hogue, C. J. Ray, D. E. Kirschner, A methodology for performing global uncertainty and sensitivity analysis in systems biology, *J. Theor. Biol.*, **254** (2008), 178–196.

36. Y. Yuan, L. J. S. Allen, Stochastic models for virus and immune system dynamics, *Math. Biosci.*, **234** (2011), 84–94.


AIMS Press